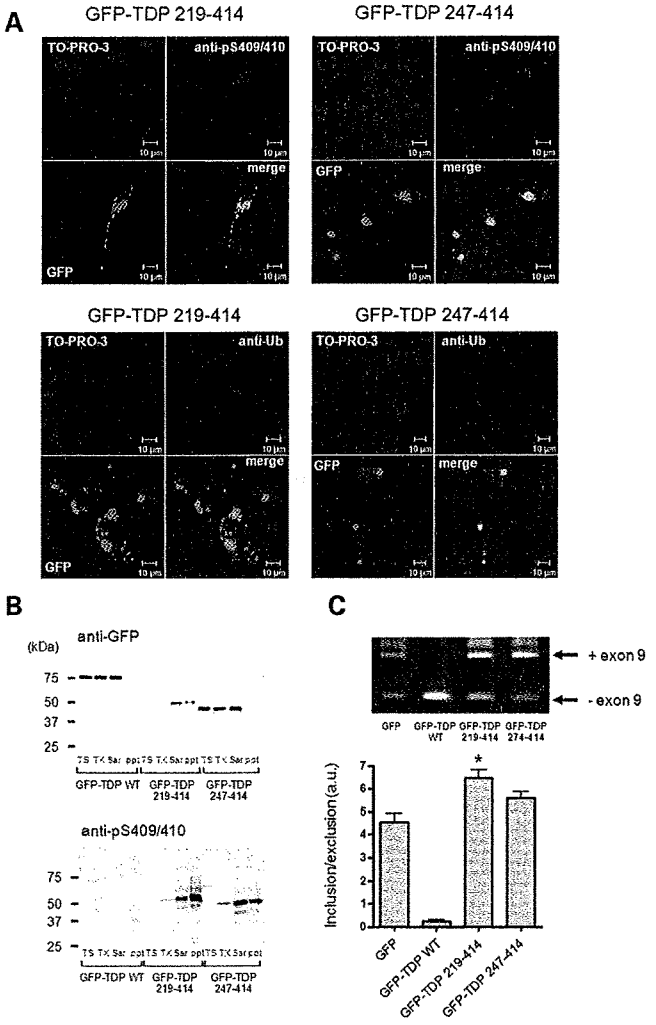

Figure 10. Pathological characterization of C-terminal fragments of TDP-43 identified in FTLD-U brains. (**A**) Confocal microscopic analyses of cells expressing GFP-TDP 219–414 (left) and GFP-TDP 247–414 (right). SH-SY5Y cells 72 h post-transfection with GFP-TDP 219–414 and GFP-TDP 247–414 were stained with anti-pS409/410 (upper) and anti-Ub (lower). (**B**) Immunoblot analyses of cells expressing GFP-TDP 219–414 and GFP-TDP 247–414. SH-SY5Y cells, 72 h post-transfection, were sequentially extracted with Tris-saline (TS), 1% Triton X-100 (TX) and 1% Sarkosyl (Sar), and the supernatants and the Sarkosyl-insoluble pellets (ppt) were subjected to SDS–PAGE. Bands were transferred to PVDF membrane and probed with anti-GFP antibody and anti-pS409/410 antibody. (**C**) CFTR exon 9 splicing assay. Gel electrophoresis of RT–PCR products of RNA from transfected cos-7 cells. The RNAs from cos-7 cells, co-transfected with the reporter plasmid pSPL3-CFTR exon 9 (TG13T5) plus pEGFP-TDP-43 expression vectors, were used as templates for RT–PCR analysis. The products were analyzed by electrophoresis in 1.5% agarose gel. The lower panel shows quantitative analyses of the ratio of CFTR exon 9 inclusion/exclusion. The intensity of each band was analysed using the Image J software. Data ($n = 4$) are means $\pm$ SEM. $^*P < 0.05$ by Student's t-test against the value of GFP.

Several groups have recently reported increased accumulation of TDP-43 fragments in the brain homogenates (8) and cultured cells (5,6) in some of the pathogenic mutations in ALS. The major component of abnormally accumulated TDP-43 is the C-terminal fragments in all TDP-43 proteinopathy (15,23). In this study, however, immunoblot analyses using a commercial TDP-43 antibody and our C-terminal 405–414 antibody (15,19) failed to show any significant differences in the generation of fragments of TDP-43 with or without various mutations (Supplementary Material, Fig. S3). The results of this study provide evidence, for the first time, that all 14 mutations tested consistently enhance aggregation of TDP-43 if they are present in the C-terminal fragments. We examined the effects of TDP-43 mutations on aggregates formation of both GFP-TDP 162–414 and GFP-TDP 218–414. We found that mutations significantly facilitate the formation of cytoplasmic inclusions of GFP-TDP 162–414, but not GFP-TDP 218–414 (data not shown). In this study, GFP-TDP 218–414 was found to be most prone to aggregate in SH-SY5Y cells. Thus, it seems likely that the high propensity to aggregate formation of GFP-TDP 218–414 may mask mutation effects on aggregates formation of GFP-TDP 218–414. So, we speculate that mutation effects were significantly detected in the experiments using GFP-TDP 162–414 which was less prone to form cytoplasmic inclusions than GFP-TDP 218–414. It seems reasonable to speculate that pathogenic mutations and N-terminal truncation synergistically promote abnormal accumulation of TDP-43. Failure to form aggregates in cells that express mutated full length TDP-43 suggests that the cell culture models recapitulate *in vivo* diseases only partially and that such models need N-terminal truncation of TDP-43 as a prerequisite for the mutation effect.

Igaz *et al.* (27) reported the cleavage site at Arg 208 in a pathological TDP-43 C-terminal fragment from FTLD-U brains and inclusion formation in cultured cells expressing resultant C-terminal fragment (residues 208–414). In the present study, by mass spectrometric analysis of the sarkosyl-insoluble fraction extracted from the FTLD-U brains, we newly identified two C-terminal fragments generated by N-terminal truncation at Asp219 and Asp247 of TDP-43 (196 and 168 amino acids, respectively). It should be noted that of these, the fragment cleaved at Asp219 (residues 219–414) is almost identical to TDP 218–414 employed in this study, which we found to be the most prone to aggregate in SH-SY5Y cells. We also confirmed that phosphorylated and ubiquitinated cytoplasmic inclusions were formed in cells expressing GFP-TDP 219–414 or GFP-TDP 247–414. Thus, the generation of aggregation-prone fragments of TDP-43 may play an important role for pathological process of TDP-43 proteinopathy. The N-termini of both identified peptides were Asp residue, suggesting that the protease(s) responsible for the cleavage may show specificity for the N-terminal side of Asp residues. Regarding the protease to degrade TDP-43, Zhang *et al.* (28) previously reported the occurrence of caspase cleavage of TDP-43 in cultured cells by the knockdown of progranulin gene. Furthermore, they recently reported the formation of intracellular inclusions immunopositive for phosphorylated TDP-43 and ubiquitin in cells expressing the GFP-tagged C-terminal fragment of TDP-43 (residues 220–414), which is expected to be generated by caspase cleavage (29). In the present study, however, we did not detect VFIPKPFR (residues 220–227), which is predicted to be produced by trypsin digestion of caspase-cleaved TDP-43, in the sarkosyl-insoluble fraction from the FTLD-U brains. These results suggest that caspase may not be the responsible enzyme for generation of

C-terminal fragments of TDP-43 in human brains. Since several abnormal fragments of 18–26 kDa were detected in FTLD-U and ALS with the antibodies to C-terminal region of TDP-43 like anti-pS409/410 (15, 19, 23), it seems reasonable to speculate the presence of the multiple cleavage sites in the middle of TDP-43. Thus, there may be other fragments, the N-termini of which have yet to be identified, and its responsible proteases. Further investigation of the degradation mechanism of TDP-43 might be needed to elucidate the pathogenesis of TDP-43 proteinopathy.

Our findings here provide further support for the idea that accumulation of fragmented TDP-43 plays an important role in TDP-43 proteinopathy. Our cellular models are expected to be useful tools to investigate the pathogenesis of TDP-43 proteinopathy, since they show pathological and biochemical characteristics similar to those of inclusions found in brains of patients, in terms of size, abnormal phosphorylation and ubiquitination.

MATERIALS AND METHODS

Construction of plasmids

To construct N-terminally green fluorescent protein (GFP)- and DsRed-fused TDP-43, a cDNA encoding full-length TDP-43 was amplified from pcDNA3-TDP-43 using the following primers: GFP/DsRed-forward, 5′-CCGCTCGAGCTATGTCTGAATATATTCGGGTAACCGAA-3′; GFP/DsRed-reverse, 5′-CGGGATCCCTACATTCCCCAGCCAGAAG-3′. The amplified fragment was digested with *Xho*I/*Bam*HI and was cloned into the same cleavage sites of the pEGFP-C1 vector (Clontech) and pDsRed-Monomer-C1 vector (Clontech), respectively. For the construction of GFP-tagged TDP-43 fragments, each fragment was amplified by PCR using the following primers: for GFP-tagged TDP-43 fragment of residues 162–414 (GFP-TDP 162–414), forward, 5′-CCGCTCGAGCTATGTCACAGCGACATATGA-3′ and GFP/DsRed-reverse; for GFP-TDP 218–414, forward, 5′-CCGCTCGAGCTATGGATGTCTTCATCCCCA-3′ and GFP/DsRed-reverse; for GFP-TDP 219–414, forward, 5′-CCGCTCGAGCT GATGTCTTCATCCCCAAGCC-3′ and GFP/DsRed-reverse; for GFP-TDP 247–414, forward, 5′-CCGCTCGAGCT GACTTGATCATTAAAGGAAT-3′ and GFP/DsRed-reverse; for GFP-TDP 274–414, forward, 5′-CCGCTCGAGCTGGAAGATTTGGTGGTAATCCA-3′ and GFP/DsRed-reverse; for GFP-TDP 315–414, forward, 5′-CCGCTCGAGCTGCGTTCAGCATTAATCCAGCCAT-3′ and GFP/DsRed-reverse; for GFP-TDP 1–161, GFP/DsRed-forward and reverse, 5′-CGGGATCCCTATACTTTCACTTGTGTTT-3′; for GFP-TDP 1–217, GFP/DsRed-forward and reverse, 5′-CGGGATCCCTACACATCCCCGTACTGAG-3′; for GFP-TDP 1–273, GFP/DsRed-forward and reverse, 5′-CGGGATCCCTAACTTCTTTCTAACTGTCTATTGCT-3′; for GFP-TDP 1–314, GFP/DsRed-forward and reverse, 5′-CGGGATCCCTAACCAAAGTTCATCCCACCACCCAT-3′. The resulting products were digested with *Xho*I/*Bam*HI and were cloned into the same cleavage sites of the pEGFP-C1 vector (Clontech). Site-directed mutagenesis of GFP-tagged or non-tagged full-length TDP-43 and GFP-tagged C-terminal fragment (GFP-TDP 162–414) was carried out to substitute Asp169 to Gly (D169G), Gly287 to Ser (G287S), Gly290 to Ala (G290A), Gly294 to Ala (G294A), Gly298 to Ser (G298S), Ala315 to Thr (A315T), Gln331 to Lys (Q331K), Met337 to Val (M337V), Gln343 to Arg (Q343R), Gly348 to Cys (G348C), Arg361 to Ser (R361S), Ala382 to Thr (A382T), Asn390 to Asp (N390D) and Asn390 to Ser (N390S) using a site-directed mutagenesis kit (Strategene). All constructs were verified by DNA sequencing.

Antibodies

A polyclonal TDP-43 antibody 10782-1-AP (anti-TDP-43) was purchased from ProteinTech Group Inc. A polyclonal antibody specific for phosphorylated TDP-43 (anti-pS409/410) and anti-405-414 antibody specific for C-terminal TDP-43 were prepared as described (15,19). Anti-ubiquitin monoclonal antibody (mAb), MAB1510, was purchased from Chemicon. Anti-GFP mAb, anti-RFP polyclonal antibody and agarose-conjugated anti-GFP were purchased from MBL (Nagoya, Japan). Monoclonal anti-alpha-tubulin and anti-p84 were obtained from Sigma and Abcam, respectively.

Cell culture and expression of plasmids

SH-SY5Y cells were cultured in DMEM/F12 medium (Sigma) supplemented with 10% (v/v) fetal calf serum, penicillin–streptomycin–glutamine (Gibco), and MEM Non-Essential Amino Acids Solution (Gibco). The cells were maintained at 37°C under a humidified atmosphere of 5% (v/v) CO_2. They were grown to 50% confluence in six-well culture dishes for transient expression and then transfected with expression plasmids using FuGENE6 (Roche) according to the manufacturer's instructions. Under our experimental conditions, the efficiency of transfection with pEGFP-C1 vector was 20–30%.

Confocal immunofluorescence microscopy

SH-SY5Y cells were grown on a coverslip (15 × 15 mm) and transfected with expression vector(s) (1 or 2 μg). After incubation for the indicated time, the transfected cells on the coverslips were fixed with 4% (w/v) paraformaldehyde in phosphate-buffered saline (PBS) for 30 min. The coverslips were then incubated in 50 mM NH_4Cl in PBS for 10 min and cell permeabilization was performed with 0.2% (v/v) Triton X-100 in PBS for 10 min. After blocking for 30 min in 5% (w/v) BSA in PBS, cells were incubated with anti-phosphorylated TDP-43 antibody, anti-pS409/410 (1:500 dilution) and anti-Ub (1:500) for 1 h at 37°C, followed by Alexa Fluor 488- or Alexa Fluor 568-labeled goat anti-rabbit or-mouse IgG (Invitrogen, 1:1000 dilution) for 1 h at 37°C. After washing, the cells were further incubated with TO-PRO-3 (Invitrogen, 1:3000 dilution in PBS) for 1 h at 37°C to stain nuclear DNA, and analyzed using an LSM5 Pascal confocal laser microscope (Carl Zeiss).

Intracellular aggregates of GFP-tagged TDP-43 fragments had much more intense fluorescence of GFP than diffusely expressed, GFP-tagged wild-type TDP-43 or GFP alone. Therefore, to quantify the cells with GFP-tagged TDP-43 aggregates, the laser power (at 488 nm for detection of GFP) was adjusted so that only the aggregates were detected (30).

Total intensity of GFP fluorescence detected at the threshold laser power and that of TO-PRO-3 fluorescence, the latter corresponding to the total number of cells, in a given field (~800 × 800 μm) were measured with LSM5 Pascal v 4.0 software (Carl Zeiss) and the ratios of cells with inclusions were calculated.

In the co-expression experiments with combinations of GFP-tagged TDP 162–414 or TDP 218–414 and DsRed-tagged wild-type TDP-43, the laser power (at 543 nm for detection of DsRed) was appropriately adjusted so that the signals did not overlap.

Sequential extraction of proteins and immunoblotting

SH-SY5Y cells were grown in six-well plates and transfected transiently with expression plasmids (1 μg). After incubation for the indicated time, cells were harvested and lysed in TS buffer [50 mM Tris–HCl buffer, pH 7.5, 0.15 M NaCl, 5 mM ethylenediaminetetraacetic acid (EDTA), 5 mM ethylene glycol bis (β-aminoethyl ether)-*N,N,N,N*-tetraacetic acid (EGTA) and protease inhibitor cocktail (Roche)]. The lysates were centrifuged at 290 000*g* for 20 min at 4°C, and the supernatant was recovered as the TS-soluble fraction. The TS-insoluble pellets were lysed in TS buffer containing 1% (v/v) Triton X-100 (TX) and centrifuged at 290 000*g* for 20 min at 4°C. The supernatant was collected as the TX-soluble fraction. The TX-insoluble pellets were further sonicated in TS buffer containing 1% (w/v) Sarkosyl (Sar) and incubated for 30 min at 37°C. The mixtures were centrifuged at 290 000*g* for 20 min at room temperature and the supernatant was recovered as the Sar-soluble fraction. The remaining pellets (insoluble in Sar) were lysed in SDS-sample buffer and heated for 5 min.

Subcellular fractionation was performed using NE-PER nuclear and cytoplasmic extraction reagents (Pierce) according to the manufacturer's instructions. SH-SY5Y cells were grown in six-well plates and transfected transiently with expression plasmids (1 μg). After incubation for 48 h, cells were harvested and fractionated into nuclear and cytoplasmic fraction using NE-PER.

Protein concentration was estimated using the BCA Protein Assay Kit (Pierce). Each sample (10 or 20 μg) was separated by 10 or 12% (v/v) SDS–PAGE using Tris–glycine buffer system, and proteins were transferred onto polyvinylidene difluoride membrane (Millipore). The blots were blocked with 3% (v/v) gelatin and incubated overnight with the indicated primary antibody in 10% (v/v) calf serum at an appropriate dilution (1:1000–5000) at room temperature. The membranes were washed and then incubated with a biotin-labeled secondary antibody (Vector) for 2 h or a horse radish peroxidase-labeled secondary antibody (BIO-RAD) for 1 h at room temperature. Signals were detected using the ABC staining kit (Vector) or ECL Plus Western Blotting Detection System (GE Healthcare).

CFTR exon 9 skipping assay

Cos-7 cells grown in six-well plates were transfected with 0.5 μg of the reporter plasmid pSPL3-CFTR9 (including a TG11T7 (16) or TG13T5 sequence) plus 1 μg of pEGFP plasmid encoding wild-type TDP-43 or its fragment, using FuGENE6. The cells were harvested 48 h post-transfection and total RNA was extracted with TRIzol (Invitrogen). The cDNA was synthesized from 1 μg of total RNA with the use of the Superscript II system (Invitrogen). Primary and secondary PCRs were carried out according to the instruction manual of the exon trapping system (Life Technologies).

Immunoprecipitation

SH-SY5Y cells grown in six-well plates were transfected with expression vectors (total 2 μg). After incubation for 3 days, cells were harvested and lysed in RIPA buffer [50 mM Tris–HCl buffer, pH 7.5, 0.15 M NaCl, 1% NP-40, 0.5% deoxycholic acid Na, 0.1% SDS, 5 mM EDTA, 5 mM EGTA, 1 mM PMSF and protease inhibitor cocktail (Roche)]. The lysates were centrifuged at 20 400*g* for 10 min at 4°C and the supernatant (total protein: ~100 μg) was recovered and subjected to IP with agarose conjugated anti-GFP [20 μl of 50% gel slurry (~5 μg of anti-GFP), MBL]. Bound proteins were washed with RIPA buffer and then eluted from the beads with SDS sample buffer. Each sample was separated by 10% SDS–PAGE and immunoblotted with anti-GFP mAb (MBL), anti-RFP polyclonal antibody (MBL) and anti-TDP-43 (ProteinTech).

Mass spectrometric analysis of C-terminal fragments of TDP-43

Sarkosyl-insoluble, 8 M urea soluble fractions prepared from the brain of patients with FTLD-U were subjected to reversed phase-HPLC on an Aquapore RP-300 column (4.6 × 30 mm, Brownlee columns) and fractionated samples were immunoblotted with anti-pS409/410. The positive fraction was lyophilized, treated with SDS-sample buffer and loaded on 15% SDS–PAGE. The pS409/410-positive ~23 kDa bands (Fig. 9A) were dissected and digested in-gel with trypsin. The digests were applied to the Paradigm MS4 HPLC system (Microm BioResources). A reversed phase capillary column (Develosil ODS-HG5, 0.075 × 150 mm, Nomura Chemical) was used at a flow rate of 300 nm/min with a 4–80% linear gradient of acetonitrile in 0.1% formic acid. Eluted peptides were directly detected with an ion trap mass spectrometer, LXQ (Thermo Electron). The obtained spectra were analyzed with BioWorks (Thermo Electron) and Mascot (Matrix Science).

Statistical analysis

The *P*-values for the description of the statistical significance of differences were calculated by means of the unpaired, two-tailed Student's *t*-test using Prism 4 software.

SUPPLEMENTARY MATERIAL

Supplementary Material is available at *HMG* online.

ACKNOWLEDGEMENTS

We thank Dr H. Mimuro (University of Tokyo) for helpful advice and discussions.

Conflict of Interest statement. None declared.

FUNDING

This work was supported by a Grant-in-Aid for Scientific Research on Priority Areas–Research on Pathomechanisms of Brain Disorders (to M.H., 20023038), and Grants-in-Aid for Scientific Research to M.H. (18300117) and F.K. (20300144) and to T.N. (19590297) and T.A. (19591024) from the Ministry of Education, Culture, Sports, Science and Technology of Japan.

REFERENCES

1. Snowden, J.S., Neary, D. and Mann, D.M. (2002) Frontotemporal dementia. *Br. J. Psychiatry.*, **180**, 140–143.
2. Arai, T., Hasegawa, M., Akiyama, H., Ikeda, K., Nonaka, T., Mori, H., Mann, D., Tsuchiya, K., Yoshida, M., Hashizume, Y. *et al.* (2006) TDP-43 is a component of ubiquitin-positive tau-negative inclusions in frontotemporal lobar degeneration and amyotrophic lateral sclerosis. *Biochem. Biophys. Res. Commun.*, **351**, 602–611.
3. Neumann, M., Sampathu, D.M., Kwong, L.K., Truax, A.C., Micsenyi, M.C., Chou, T.T., Bruce, J., Schuck, T., Grossman, M., Clark, C.M. *et al.* (2006) Ubiquitinated TDP-43 in frontotemporal lobar degeneration and amyotrophic lateral sclerosis. *Science*, **314**, 130–133.
4. Gitcho, M.A., Baloh, R.H., Chakraverty, S., Mayo, K., Norton, J.B., Levitch, D., Hatanpaa, K.J., White, C.L. III, Bigio, E.H., Caselli, R. *et al.* (2008) TDP-43 A315T mutation in familial motor neuron disease. *Ann. Neurol.*, **63**, 535–538.
5. Kabashi, E., Valdmanis, P.N., Dion, P., Spiegelman, D., McConkey, B.J., Vande Velde, C., Bouchard, J.P., Lacomblez, L., Pochigaeva, K., Salachas, F. *et al.* (2008) TARDBP mutations in individuals with sporadic and familial amyotrophic lateral sclerosis. *Nat. Genet.*, **40**, 572–574.
6. Sreedharan, J., Blair, I.P., Tripathi, V.B., Hu, X., Vance, C., Rogelj, B., Ackerley, S., Durnall, J.C., Williams, K.L., Buratti, E. *et al.* (2008) TDP-43 mutations in familial and sporadic amyotrophic lateral sclerosis. *Science*, **319**, 1668–1672.
7. Van Deerlin, V.M., Leverenz, J.B., Bekris, L.M., Bird, T.D., Yuan, W., Elman, L.B., Clay, D., Wood, E.M., Chen-Plotkin, A.S., Martinez-Lage, M. *et al.* (2008) TARDBP mutations in amyotrophic lateral sclerosis with TDP-43 neuropathology: a genetic and histopathological analysis. *Lancet. Neurol.*, **7**, 409–416.
8. Yokoseki, A., Shiga, A., Tan, C.F., Tagawa, A., Kaneko, H., Koyama, A., Eguchi, H., Tsujino, A., Ikeuchi, T., Kakita, A. *et al.* (2008) TDP-43 mutation in familial amyotrophic lateral sclerosis. *Ann. Neurol.*, **63**, 538–542.
9. Benajiba, L., Le Ber, I., Camuzat, A., Lacoste, M., Thomas-Anterion, C., Couratier, P., Legallic, S., Salachas, F., Hannequin, D., Decousus, M. *et al.* (2009) TARDBP mutations in motoneuron disease with frontotemporal lobar degeneration. *Ann. Neurol.*, **65**, 470–473.
10. Deng, H.X., Hentati, A., Tainer, J.A., Iqbal, Z., Cayabyab, A., Hung, W.Y., Getzoff, E.D., Hu, P., Herzfeldt, B., Roos, R.P. *et al.* (1993) Amyotrophic lateral sclerosis and structural defects in Cu,Zn superoxide dismutase. *Science*, **261**, 1047–1051.
11. Rosen, D.R., Siddique, T., Patterson, D., Figlewicz, D.A., Sapp, P., Hentati, A., Donaldson, D., Goto, J., O'Regan, J.P., Deng, H.X. *et al.* (1993) Mutations in Cu/Zn superoxide dismutase gene are associated with familial amyotrophic lateral sclerosis. *Nature*, **362**, 59–62.
12. Mackenzie, I.R., Bigio, E.H., Ince, P.G., Geser, F., Neumann, M., Cairns, N.J., Kwong, L.K., Forman, M.S., Ravits, J., Stewart, H. *et al.* (2007) Pathological TDP-43 distinguishes sporadic amyotrophic lateral sclerosis from amyotrophic lateral sclerosis with SOD1 mutations. *Ann. Neurol.*, **61**, 427–434.
13. Tan, C.F., Eguchi, H., Tagawa, A., Onodera, O., Iwasaki, T., Tsujino, A., Nishizawa, M., Kakita, A. and Takahashi, H. (2007) TDP-43 immunoreactivity in neuronal inclusions in familial amyotrophic lateral sclerosis with or without SOD1 gene mutation. *Acta. Neuropathol.*, **113**, 535–542.
14. Piao, Y.S., Wakabayashi, K., Kakita, A., Yamada, M., Hayashi, S., Morita, T., Ikuta, F., Oyanagi, K. and Takahashi, H. (2003) Neuropathology with clinical correlations of sporadic amyotrophic lateral sclerosis: 102 autopsy cases examined between 1962 and 2000. *Brain Pathol.*, **13**, 10–22.
15. Hasegawa, M., Arai, T., Nonaka, T., Kametani, F., Yoshida, M., Hashizume, Y., Beach, T.G., Buratti, E., Baralle, F., Morita, M. *et al.* (2008) Phosphorylated TDP-43 in frontotemporal lobar degeneration and amyotrophic lateral sclerosis. *Ann. Neurol.*, **64**, 60–70.
16. Nonaka, T., Arai, T., Buratti, E., Baralle, F.E., Akiyama, H. and Hasegawa, M. (2009) Phosphorylated and ubiquitinated TDP-43 pathological inclusions in ALS and FTLD-U are recapitulated in SH-SY5Y cells. *FEBS Lett.*, **583**, 394–400.
17. Winton, M.J., Igaz, L.M., Wong, M.M., Kwong, L.K., Trojanowski, J.Q. and Lee, V.M. (2008) Disturbance of nuclear and cytoplasmic TAR DNA-binding protein (TDP-43) induces disease-like redistribution, sequestration, and aggregate formation. *J. Biol. Chem.*, **283**, 13302–13309.
18. Ayala, Y.M., Zago, P., D'Ambrogio, A., Xu, Y.F., Petrucelli, L., Buratti, E. and Baralle, F.E. (2008) Structural determinants of the cellular localization and shuttling of TDP-43. *J. Cell Sci.*, **121**, 3778–3785.
19. Inukai, Y., Nonaka, T., Arai, T., Yoshida, M., Hashizume, Y., Beach, T.G., Buratti, E., Baralle, F.E., Akiyama, H., Hisanaga, S.I. *et al.* (2008) Abnormal phosphorylation of Ser409/410 of TDP-43 in FTLD-U and ALS. *FEBS Lett.*, **582**, 2899–2904.
20. Buratti, E., Dork, T., Zuccato, E., Pagani, F., Romano, M. and Baralle, F.E. (2001) Nuclear factor TDP-43 and SR proteins promote *in vitro* and *in vivo* CFTR exon 9 skipping. *EMBO J.*, **20**, 1774–1784.
21. Buratti, E. and Baralle, F.E. (2001) Characterization and functional implications of the RNA binding properties of nuclear factor TDP-43, a novel splicing regulator of CFTR exon 9. *J. Biol. Chem.*, **276**, 36337–36343.
22. Johnson, B.S., McCaffery, J.M., Lindquist, S. and Gitler, A.D. (2008) A yeast TDP-43 proteinopathy model: Exploring the molecular determinants of TDP-43 aggregation and cellular toxicity. *Proc. Natl Acad. Sci. USA*, **105**, 6439–6444.
23. Igaz, L.M., Kwong, L.K., Xu, Y., Truax, A.C., Uryu, K., Neumann, M., Clark, C.M., Elman, L.B., Miller, B.L., Grossman, M. *et al.* (2008) Enrichment of C-terminal fragments in TAR DNA-binding protein-43 cytoplasmic inclusions in brain but not in spinal cord of frontotemporal lobar degeneration and amyotrophic lateral sclerosis. *Am. J. Pathol.*, **173**, 182–194.
24. Buratti, E., Brindisi, A., Giombi, M., Tisminetzky, S., Ayala, Y.M. and Baralle, F.E. (2005) TDP-43 binds heterogeneous nuclear ribonucleoprotein A/B through its C-terminal tail: an important region for the inhibition of cystic fibrosis transmembrane conductance regulator exon 9 splicing. *J. Biol. Chem.*, **280**, 37572–37584.
25. Ayala, Y.M., Pantano, S., D'Ambrogio, A., Buratti, E., Brindisi, A., Marchetti, C., Romano, M. and Baralle, F.E. (2005) Human, Drosophila, and C.elegans TDP43: nucleic acid binding properties and splicing regulatory function. *J. Mol. Biol.*, **348**, 575–588.
26. Wang, H.Y., Wang, I.F., Bose, J. and Shen, C.K. (2004) Structural diversity and functional implications of the eukaryotic TDP gene family. *Genomics*, **83**, 130–139.
27. Igaz, L.M., Kwong, L.K., Chen-Plotkin, A., Winton, M.J., Unger, T.L., Xu, Y., Neumann, M., Trojanowski, J.Q. and Lee, V.M. (2009) Expression Of TDP-43 C-terminal fragments in vitro recapitulates pathological features of TDP-43 proteinopathies. *J. Biol. Chem.*, **284**, 8516–8524.
28. Zhang, Y.J., Xu, Y.F., Dickey, C.A., Buratti, E., Baralle, F., Bailey, R., Pickering-Brown, S., Dickson, D. and Petrucelli, L. (2007) Progranulin mediates caspase-dependent cleavage of TAR DNA binding protein-43. *J. Neurosci.*, **27**, 10530–10534.
29. Zhang, Y.J., Xu, Y.F., Cook, C., Gendron, T.F., Roettges, P., Link, C.D., Lin, W.L., Tong, J., Castanedes-Casey, M., Ash, P. *et al.* (2009) Aberrant cleavage of TDP-43 enhances aggregation and cellular toxicity. *Proc. Natl Acad. Sci. USA*, **106**, 7607–7612.
30. Nagai, Y., Tucker, T., Ren, H., Kenan, D.J., Henderson, B.S., Keene, J.D., Strittmatter, W.J. and Burke, J.R. (2000) Inhibition of polyglutamine protein aggregation and cell death by novel peptides identified by phage display screening. *J. Biol. Chem.*, **275**, 10437–10442.

A Cellular Model To Monitor Proteasome Dysfunction by α-Synuclein

Takashi Nonaka* and Masato Hasegawa*

Department of Molecular Neurobiology, Tokyo Institute of Psychiatry, Tokyo Metropolitan Organization for Medical Research, 2-1-8 Kamikitazawa, Setagaya-ku, Tokyo 156-8585

Biochemistry®

Reprint from
Volume 48, Number 33, Pages 8014–8022

8014 *Biochemistry* **2009,** *48,* 8014–8022
DOI: 10.1021/bi900619j

BIOCHEMISTRY
including biophysical chemistry & molecular biology
Article

A Cellular Model To Monitor Proteasome Dysfunction by α-Synuclein†

Takashi Nonaka* and Masato Hasegawa*

Department of Molecular Neurobiology, Tokyo Institute of Psychiatry, Tokyo Metropolitan Organization for Medical Research, 2-1-8 Kamikitazawa, Setagaya-ku, Tokyo 156-8585.

Received April 9, 2009; Revised Manuscript Received June 16, 2009

ABSTRACT: Impairment of the ubiquitin-proteasome degradation system has recently been suggested to be related to the onset of neurodegenerative disorders such as Alzheimer's disease and Parkinson's disease. In this study, we investigated whether intracellular α-synuclein affects proteasome activity in SH-SY5Y cells. To monitor intracellular proteasome activity, we used a reporter consisting of a short peptide degron fused to the carboxyl-terminus of green fluorescent protein (GFP-CL1), which is known to be degraded by proteasome. The level of intact GFP-CL1 was dramatically increased by coexpression of GFP-CL1 and α-synuclein, as judged by confocal microscopic and immunoblot analyses. Expression of two pathogenic mutants of α-synuclein, A30P and A53T, and phosphomimetic S129D mutant increased the intensities of GFP more effectively than did wild-type α-synuclein. GFP fluorescence in cells transfected with Δ73-83 mutant or β-synuclein, which does not assemble into filaments *in vitro*, was not changed as compared with that in cells expressing GFP-CL1 alone. Thus, the ability of α-synuclein to inhibit proteasome activity is related to its propensity to assemble into filaments. Furthermore, we observed that some compounds inhibiting α-synuclein filament formation *in vitro* prevented the α-synuclein-mediated proteasome dysfunction in cells transfected with both GFP-CL1 and α-synuclein. The cellular model expressing both GFP-CL1 and α-synuclein may be a useful tool to screen compounds protecting neurons from α-synuclein-mediated proteasome dysfunction.

Parkinson's disease (PD) is one of the most common neurodegenerative disorders. It is characterized by loss of dopaminergic neurons in the substantia nigra and by intracellular inclusion bodies known as Lewy bodies and Lewy neuritis. α-Synuclein is a natively unfolded protein and is deposited in a hyperphosphorylated form as the major component of these filamentous inclusions (*1*–*3*). Genetic studies have revealed that missense mutations (A30P, E46K, and A53T) in the α-synuclein gene cause familial forms of PD and dementia with Lewy bodies (DLB) (*4*–*6*). It has also been reported that multiplications (duplication and triplication) of α-synuclein gene cause an inherited form of PD and DLB (*7*–*11*). Thus, an increased level of intracellular α-synuclein is thought to contribute to the onset of familial PD.

Intracellular and extracellular protein deposits may cause neuronal cell death and may signal onset of many neurodegenerative diseases. We have reported that phosphorylated α-synuclein is partially ubiquitinated in α-synucleinopathy brains (*12*). We also found that ubiquitination of α-synuclein occurs in cultured cells at sites identical to those of filamentous α-synuclein ubiquitinated *in vitro*, suggesting that ubiquitination may be a late event in the formation of Lewy bodies (*13*). A recent paper confirmed our findings and showed that monoubiquitination and multiubiquitination at Lys12, 21, and 23 are detectable on phosphorylated α-synuclein in α-synucleinopathy brains (*14*). These findings indicate that the ubiquitin-proteasome system (UPS) is targeted to abnormal α-synuclein in the brains of patients but that ubiquitinated α-synuclein cannot be degraded by the UPS, suggesting that the UPS may not be effective to clear the abnormal form of α-synuclein.

The UPS functions in cellular quality control by degrading misfolded, unassembled, or damaged proteins that might create toxic intracellular aggregates (*15*, *16*). As the proteasome efficiently degrades multiubiquitinated proteins, the presence of elevated levels of ubiquitin conjugates in intracellular deposits of aggregated proteins in most neurodegenerative diseases suggests a linkage between UPS dysfunction and pathogenesis. Functional relationships between α-synuclein and the UPS have been described (*17*–*19*). Synder et al. reported that aggregated and monomeric α-synuclein inhibit proteasomal function *in vitro* (*20*). Lindersson et al. also observed proteasomal inhibition by α-synuclein filaments and oligomers *in vitro* (*21*). In cultured cells, it remains controversial whether expression of α-synuclein affects intracellular proteasome activity. Martin-Clemente et al. reported that α-synuclein expression level does not significantly affect proteasome function in PC12 cells (*22*), while Fujita et al. reported that proteasome activity was significantly decreased in cells overexpressing wild-type α-synuclein (*23*). Stefanis et al. described that expression of A53T mutant, but not wild-type α-synuclein, inhibits proteasome activity in PC12 cells (*24*). It was also reported that cell-produced α-synuclein oligomers are targeted to and impair the 26S proteasome (*25*).

Recently, Bence et al. reported impairment of the ubiquitin-proteasome system by the expression of an exon 1 fragment of

†This work was supported by a Grant-in-Aid for Scientific Research on Priority Areas–Research on Pathomechanisms of Brain Disorders (to M.H., 20023038) and Grants-in-Aid for Scientific Research (B) (to M.H., 18300117) and (C) (to T.N., 19590297) from the Ministry of Education, Culture, Sports, Science and Technology of Japan.

*To whom correspondence should be addressed. Phone: +81-3-3304-5701. Fax: +81-3-3329-8035. E-mail: nonakat@prit.go.jp, masato@prit.go.jp.

 Published on Web 07/24/2009

huntingtin containing expanded polyglutamine homopolymer in cultured cells (*26*). They used a green fluorescent protein (GFP) reporter that is specifically degraded by the cellular proteasome. This fluorescent reporter system is also useful for facile detection of proteasome activity in *Caenorhabditis elegans* (*27*).

In this study, to investigate whether intracellular α-synuclein affects proteasome activity, we have established a more sensitive assay system to monitor proteasome activity in cells using the GFP reporter and demonstrated impairment of proteasome function by expression of α-synuclein in SH-SY5Y cells. We also found that two pathogenic mutations of α-synuclein (A30P and A53T) and S129D mutant, which mimics phosphorylation, inhibit proteasome activity more effectively than does wild-type α-synuclein, while Δ73-83 mutant and β-synuclein, which do not form fibrils *in vitro*, do not affect proteasome function. Furthermore, we used our cellular model to screen for compounds protecting cells from proteasome inhibition by α-synuclein and found that some polyphenols attenuate α-synuclein-induced proteasome impairment.

EXPERIMENTAL PROCEDURES

Construction of Plasmids. The GFP-CL1 plasmid was constructed by digestion of pEGFP-C1 (Clontech) with *Bgl*II and *Sal*I and ligation with hybridized oligonucleotides termed CL1s (5′-GATCCGCTTGTAAAAATTGGTTTTCTTCTTT-ATCTCATTTTGTTATTCATTTATAAG-3′) and CL1a (5′-TCGACTTATAAATGAATAACAAAATGAGATAAAGA-AGAAAACCAATTTTTACAAGCG-3′). The resulting construct, the GFP gene containing an oligonucleotide encoding ACKNWFSSLSHFVIHL, was confirmed by DNA sequencing and designated pEGFP-CL1.

Human α-synuclein, β-synuclein, tau 3R1N, and 4R1N cDNAs in pRK172 vector were kind gifts from Dr. M. Goedert. The open reading frames of α-synuclein, β-synuclein, tau 3R1N, and 4R1N were subcloned into the mammalian expression vector pcDNA3. To construct plasmids encoding α-synuclein mutants A30P, A53T, S129A, and S129D, we performed site-directed mutagenesis using a site-directed mutagenesis kit (Strategene). We constructed a deletion mutant (residues 73−83: Δ73-83) of α-synuclein using PCR with the forward primer (5′-GGAG-CAGGGAGCATTGCAGCA-3′) and the reverse primer (5′-CGTCACCACTGCTCCTCCAAC-3′) using pcDNA3-α-synuclein as a template. The amplified fragments were self-ligated, and the resulting plasmids designated pcDNA-α-synuclein Δ73-83. All constructs were verified by DNA sequencing.

Cell Culture and Plasmid Expression. SH-SY5Y cells were cultured in DMEM/F12 medium (Sigma) supplemented with 10% (v/v) fetal calf serum, Penicillin-Streptomycin-Glutamine (GIBCO), and MEM Non-Essential Amino Acids Solution (GIBCO). The cells were maintained at 37 °C in a humidified atmosphere of 5% (v/v) CO_2. Cells were grown to 50% confluence in six-well culture dishes for transient expression and then transfected with various expression plasmids using FuGENE6 (Roche) according to the manufacturer's instructions.

Confocal Immunofluorescence Microscopy. SH-SY5Y cells were grown on a coverslip (15 mm × 15 mm) and transfected with expression vector (total 1.3 μg, e.g., 1 μg of pcDNA3-α-synuclein plus 0.3 μg of pEGFP-CL1). After incubation for indicated times, transfected cells on the coverslips were fixed with 4% (w/v) paraformaldehyde in phosphate-buffered saline (PBS) for 30 min. The coverslips were then incubated in 50 mM NH_4Cl in PBS for 10 min, and cell permeabilization was performed with 0.2% (v/v) Triton X-100 in PBS for 10 min. The cells were blocked for 30 min in 5% (w/v) BSA in PBS, then incubated with anti-α-synuclein monoclonal antibody, Syn102 (*28*) (1:500 dilution) for 1 h at 37 °C, followed by TRITC-labeled goat anti-mouse IgG (Sigma, 1:500 dilution) as the secondary antibody for 1 h at 37 °C. They were washed again and further incubated with TO-PRO-3 (Molecular Probes, 1:3000 dilution in PBS) for 45 min at 37 °C to stain nuclear DNA and analyzed using a LSM5 Pascal confocal laser microscope (Zeiss).

Sequential Extraction of Proteins and Immunoblotting. SH-SY5Y cells were grown in a six-well plate and transiently transfected with expression plasmids (total 1.3 μg). After incubation for 48−72 h, cells were harvested and lysed in TS buffer [50 mM Tris-HCl buffer, pH 7.5, 0.15 M NaCl, 5 mM ethylenediaminetetraacetic acid, 5 mM ethylene glycol bis(β-aminoethyl ether)-*N*,*N*,*N*,*N*-tetraacetic acid, and protease inhibitor cocktail (Roche)]. The lysate was centrifuged at 290,000*g* for 20 min at 4 °C, and the supernatant recovered as the TS-soluble fraction. The TS-insoluble pellet was lysed in TS buffer containing 1% (v/v) Triton X-100 (TX) and centrifuged at 290,000*g* for 20 min at 4 °C. The supernatant was collected as the TX-soluble fraction. The TX-insoluble pellet was further lyzed in SDS-sample buffer and heated for 5 min. Protein concentration was estimated by using the BCA Protein Assay Kit (Pierce). Samples (20 μg) were separated by 13.5% (v/v) SDS−PAGE using the Tris-tricine buffer system and proteins were transferred onto polyvinylidene difluoride membrane (Millipore). The blots were then blocked with 3% (v/v) gelatin and incubated overnight with anti-GFP monoclonal antibody (MBL), anti-Syn102, anti-human tau monoclonal antibody (HT7, Thermo Scientific) or anti-α-tublin monoclonal antibody (Sigma) in 10% (v/v) calf serum at a dilution of 1:1,000−5,000 at room temperature. After washing, blots were incubated with horseradish peroxidase-labeled secondary antibody (Bio-Rad) at a dilution of 1:10,000 in 10% (v/v) calf serum for 1 h at room temperature or a biotin-labeled secondary antibody (Vector) for 2 h at room temperature. Signals were detected using the chemiluminescence reagent Immunostar (Wako) or the ABC staining kit (Vector).

Measurement of Proteasome Activity Using a Peptide Substrate. SH-SY5Y cells transfected with expression plasmids were cultured for 72 h or treated with 20 μM MG132 for 6 h. Cells were harvested and cytosolic fraction was prepared as follows. Cells were resuspended in 100 μL of phosphate-buffered saline (PBS) and disrupted by sonication. Insoluble material was removed by ultracentrifugation at 290,000*g* for 20 min at 4 °C. The supernatant was assayed for proteasome activity by using a fluorescent peptide substrate, benzyloxycarbonyl-Leu-Leu-Glu-7-amido-4-methylcoumarin (z-LLE-MCA, Peptide Institute, Inc.). Aliquots (10 μL) were mixed with 0.1 M Tris-HCl buffer, pH 7.5 and water in a total volume of 1 mL. After preincubation at 37 °C for 10 min, 10 μL of 10 mM peptide substrate was added and the mixture was incubated for 30 min. A solution of 2% (v/v) acetic acid (1 mL) was added to the reaction mixture, and 7-amino-4-methylcoumarin (AMC) release was measured fluorometrically (excitation wavelength of 365 nm; emission wavelength of 460 nm). Enzyme activity was described as arbitrary unit/mg protein.

Screening for Compounds Preventing Proteasome Inhibition by α-Synuclein in Cultured Cells. SH-SY5Y cells were grown in six-well plates or on coverslips and transfected with both α-synuclein (1 μg) and GFP-CL1 plasmids (0.3 μg).

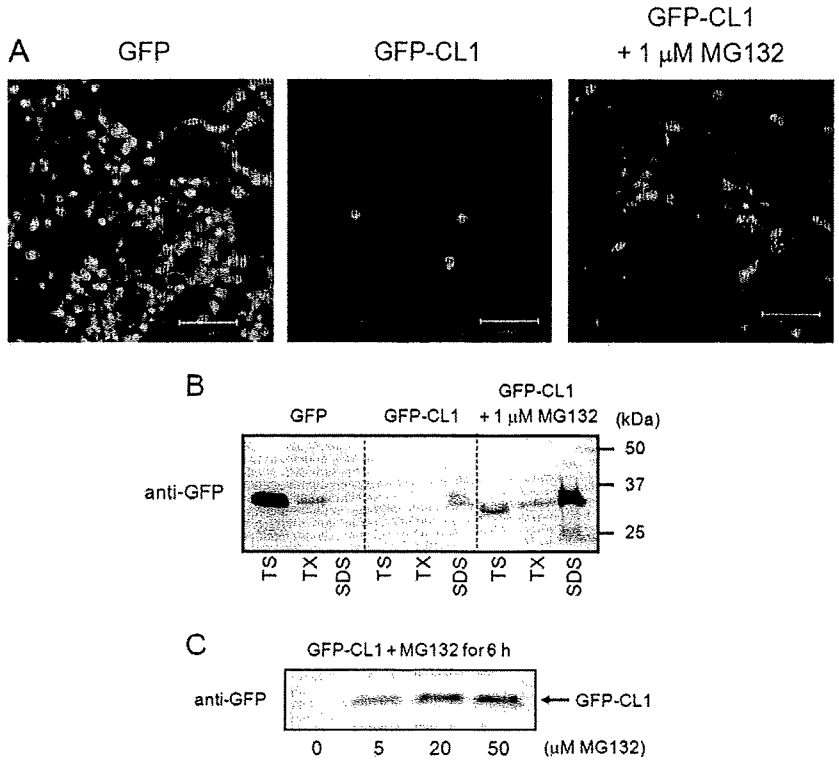

FIGURE 1: GFP-CL1 is degraded by proteasome in SH-SY5Y cells. (A) SH-SY5Y cells grown on coverslips were transfected with GFP or GFP-CL1 using FuGENE6. After an overnight incubation with or without 1 μM MG132, cells were fixed (total 48 h after transfestion), stained with TO-PRO-3 (Blue), and analyzed by confocal microscopy. Scale bar = 100 μm. (B) SH-SY5Y cells were transfected with GFP or GFP-CL1 and treated overnight with or without 1 μM MG132. Cells were harvested, and cell lysate was fractionated as described in Experimental Procedures and analyzed by immunoblotting using anti-GFP antibody. TS, Tris-soluble fraction; TX, Triton X-100-soluble fraction; SDS, SDS-soluble fraction. (C) SH-SY5Y cells were transfected with GFP-CL1 and treated with MG132 (0−50 μM) for 6 h. The cells were harvested, and the TX-insoluble fraction was analyzed by immunoblotting with anti-GFP antibody.

Various compounds (all at 40 μM) were added to the culture medium 2 h after transfection. Cells were harvested after incubation for 72 h, and the immunoblot and/or confocal microscopic analyses were performed as above. A decrease in GFP level in transfected cells treated with a compound, compared with the GFP level in transfected cells without such treatment, indicated that the compound rescues cells from proteasome dysfunction caused by expression of α-synuclein.

RESULTS

Cellular Expression of GFP-CL1. To establish a sensitive and convenient assay system for proteasome activity in cultured cells, we constructed GFP-CL1, which is GFP fused at the C-terminus with the 16-residue degron peptide CL1 (*26*, *29*). We transiently transfected SH-SY5Y cells with GFP or GFP-CL1, and analyzed the cells using confocal microscopy. As shown in Figure 1A, the fluorescence of GFP in cells transfected with GFP-CL1 was less than that in cells expressing GFP. The proteasome inhibitor MG132 increased fluorescence intensity in GFP-CL1-transfected cells (Figure 1A). Thus, we reconfirmed that the CL1 sequence specifically targeted normally stable GFP for efficient degradation by proteasome, as reported previously (*26*).

To biochemically characterize the proteasomal degradation of GFP-CL1, we fractionated lysates of cells transfected with GFP-CL1 or GFP. The TS-, TX-, and SDS-soluble fractions were analyzed by immunoblotting using anti-GFP antibody. As shown in Figure 1B, almost all GFP was recovered in the TS fraction in cells transfected with GFP, although a little GFP was detected in the TX-soluble fraction. In contrast, in cells expressing GFP-CL1, only weak GFP immunoreactivity was detected in the TS- and TX-insoluble fractions because of GFP-CL1 degradation by proteasome in transfected cells. Interestingly, in cells expressing GFP-CL1 treated with MG132, a band of uncleaved GFP-CL1 was detected in the SDS-soluble fraction in addition to the weak bands seen in the TS- and TX-soluble fractions, suggesting that uncleaved GFP-CL1 unexpectedly aggregates in cells when proteasome activity is inhibited by MG132 treatment. We also reconfirmed that MG132 treatment effectively and dose-dependently blocked the degradation of GFP-CL1 (Figure 1C).

Expression of α-Synuclein Inhibits Cellular Proteasome Activity. To investigate whether expression of α-synuclein might affect proteasome function in cultured cells, we cotransfected both α-synuclein and GFP-CL1 into SH-SY5Y cells. To reconfirm that GFP-CL1 is effectively degraded by proteasome, cells transfected with GFP-CL1 were treated with several protease inhibitors. SDS-soluble fraction of cell lysate was subjected to immunoblot analysis using anti-GFP antibody. As shown in Figure 2A, increased levels of GFP-CL1 band were observed in cells coexpressing GFP-CL1 and α-synuclein (lane 6), indicating that proteasome activity is inhibited effectively by expression of α-synuclein. Similar results were obtained when we treated cells expressing GFP-CL1 with MG132 or lactacystin (lane 3 and 4). On the other hand, leucyl-leucinal (LL, a calpain inhibitor) or chloroquine (a lysosomal inhibitor) did not inhibit GFP-CL1 degradation (lanes 2 and 5). We then tested whether the proteasome inhibition by α-synuclein is dose-dependent, i.e., dependent on the α-synuclein expression level. SH-SY5Y cells were

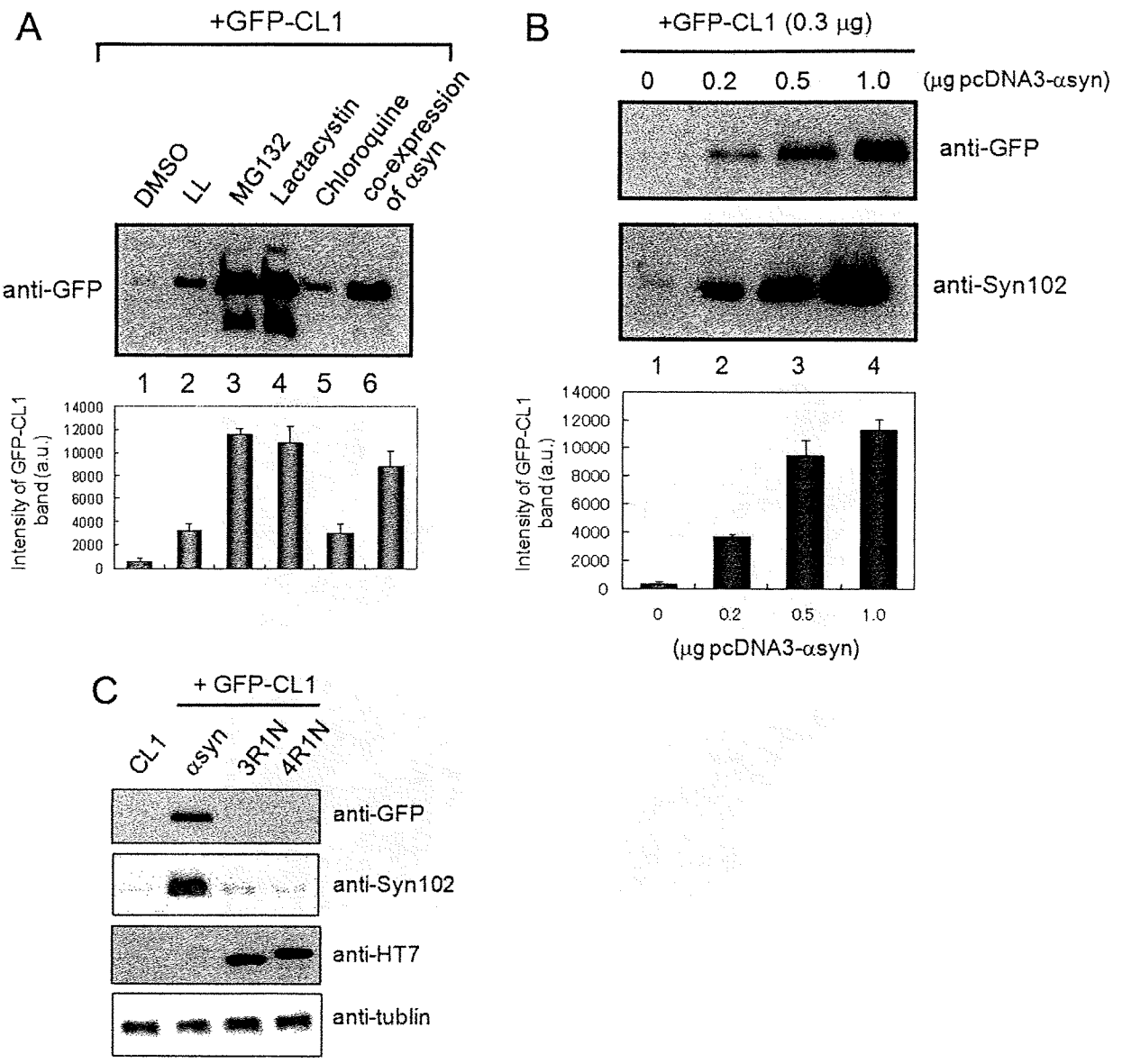

FIGURE 2: Expression of α-synuclein inhibits proteasome activity in SH-SY5Y cells. (A) SH-SY5Y cells transfected with GFP-CL1 were treated with 1 μM LL, MG132, lactacystin, and chloroquine overnight. In the case of coexpression, cells were transfected with both GFP-CL1 and α-synuclein using FuGENE6. The cells were harvested, and the Triton X-100-insoluble and SDS-soluble fractions were prepared and analyzed by immunoblotting using an anti-GFP antibody. The results of quantitative analysis of the GFP-CL1 bands, expressed as means + SD (n = 3), are shown below the blot. (B) SH-SY5Y cells were transfected with GFP-CL1 (0.3 μg), α-synuclein (0, 0.2, 0.5, or 1 μg), and/or pcDNA3 empty vector (total plasmids = 1.3 μg) and incubated for 72 h. The cells were harvested, and then Tris-soluble (lower panels) and SDS-soluble fractions (upper panels) were prepared. Immunoblot analyses were performed using anti-GFP (upper panels) or anti-Syn102 (lower panels) antibodies. The results of quantitative analysis of the GFP-CL1 bands, expressed as means + SD (n = 3), are shown below the blot. (C) SH-SY5Y cells were transfected with both GFP-CL1 (0.3 μg) and α-synuclein (1 μg) or pcDNA3-tau 3R1N or 4R1N vector (1 μg) and incubated for 72 h. The cells were harvested, and the TX-insoluble fraction was analyzed by immunoblotting with anti-GFP antibody. The TS-soluble fraction was also analyzed by using anti-Syn102, anti-HT7, and anti-tubulin antibodies (as a loading control).

transfected with both pEGFP-CL1 (0.3 μg) and pcDNA3-α-synuclein (0, 0.2, 0.5, or 1 μg; total 1.3 μg plasmids), followed by immunoblot analysis. The result showed that the level of intact GFP-CL1 increased in parallel with increased expression of α-synuclein (Figure 2B). Furthermore, we tested whether expression of tau protein which is also an effective substrate for proteasome (*30*), inhibits intracellular proteasome activity in SH-SY5Y cells. We found that expression of tau protein (3R1N and 4R1N) did not affect the proteasome activity in SH-SY5Y cells, suggesting that the effect of α-synuclein on the proteasome activity observed in this study is not simply due to overexpression of a protein, but is specific for α-synuclein. We also confirmed the absence of significant cell death in our cellular model transiently expressing α-synuclein, suggesting that the decreased proteasome activity found in cells expressing α-synuclein is not caused by cellular damage due to the toxicity of expressed α-synuclein.

To visually monitor proteasome inhibition due to expression of α-synuclein, SH-SY5Y cells were transiently cotransfected with α-synuclein and GFP-CL1, and transfected cells were analyzed by confocal microscopy. As shown in Figure 3C, the numbers of GFP-positive cells were significantly increased in cells transfected with wild-type α-synuclein and GFP-CL1, compared with cells transfected with GFP-CL1 alone (Figure 3B). This is in good agreement with the above immunoblotting data (Figure 2), indicating that expression of α-synuclein inhibited proteasome activity.

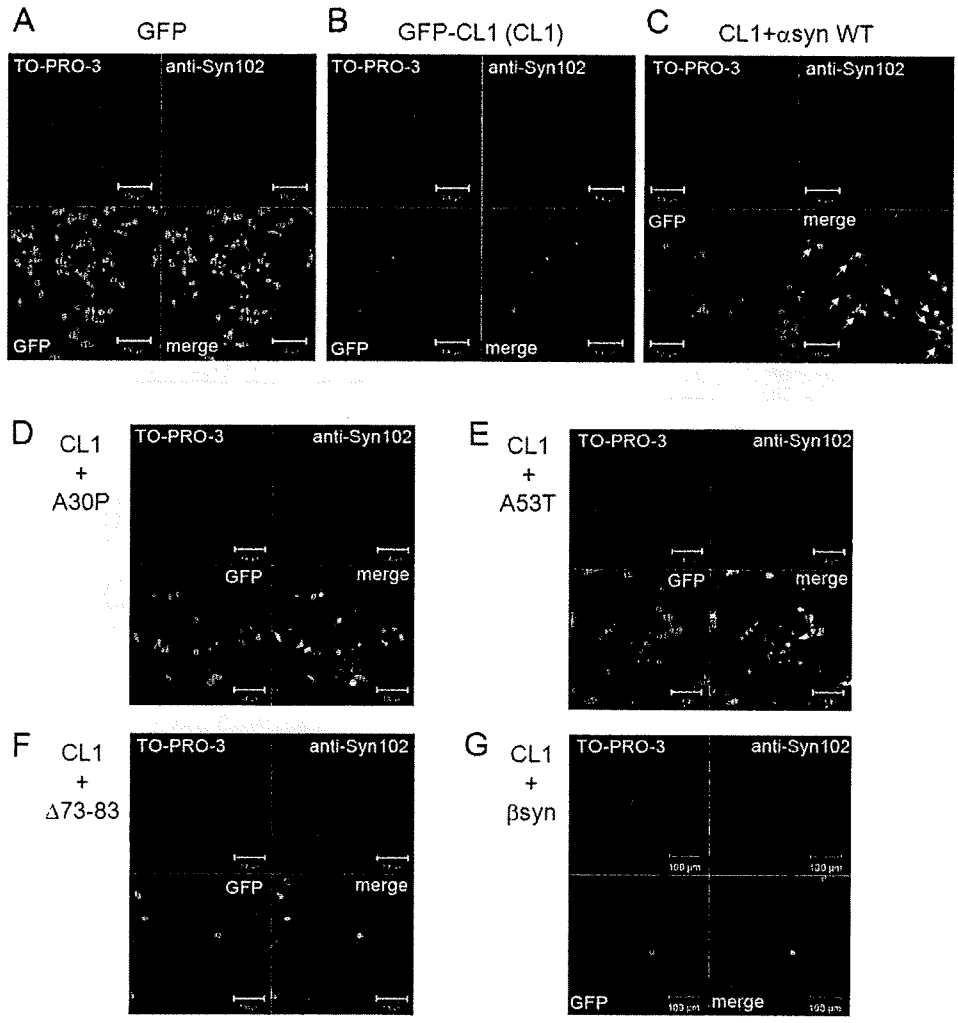

FIGURE 3: Expression of α-synuclein mutants affects proteasome activity in SH-SY5Y cells. SH-SY5Y cells grown on coverslips were transfected with GFP (A), GFP-CL1 (B), or both GFP-CL1 and wild-type α-synuclein (C), A30P (D), A53T (E), Δ73-83 (F), or β-synuclein (G). Cells were fixed 72 h after transfection and stained with anti-Syn102 (Red) and TO-PRO-3 (blue). Intracellular α-synuclein inhibits proteasome activity in cells expressing both GFP-CL1 and α-synuclein (arrows). Scale bar = 100 μm.

Taken together, these results showed that proteasome activity can be specifically and sensitively analyzed by monitoring the fluorescence intensity or immunoreactivity of GFP-CL1 in cultured cells and that the expression of α-synuclein impairs cellular proteasome function.

Effects of Expression of α-Synuclein Mutants and β-Synuclein on Proteasome Activity. Recombinant α-synuclein with a pathogenic mutation (A30P, A53T, or E46K) is more prone to assemble into filaments *in vitro* than the wild-type protein (*31*, *32*)). β-Synuclein and γ-synuclein (*33*) and the α-synuclein deletion mutant Δ73-83 (deletion of 73−83 residues) did not form fibrils *in vitro* (Nonaka et al., unpublished data). To study the effects of α-synuclein mutations on cellular proteasome activity, we transiently cotransfected these mutants and GFP-CL1 into SH-SY5Y cells and examined the cells using confocal microscopy. As shown in Figure 3, we found that increased GFP signals were observed in cells transfected with A30P (Figure 3D) or A53T (Figure 3E) compared with the signal seen in cells transfected with wild-type α-synuclein (Figure 3C), although the expression levels of the α-synuclein proteins were almost equal (Figure 3 and 4A). In contrast, little GFP fluorescence was detected in cells transfected with the α-synuclein deletion mutant Δ73-83 (Figure 3F) or β-synuclein (Figure 3G).

We also quantitatively examined the effects of these α-synuclein mutations on proteasome activity using immunoblot analysis. SH-SY5Y cells were transfected with both GFP-CL1 and wild-type α-synuclein, or the A30P, A53T, or Δ73-83 mutant, or β-synuclein. Uncleaved GFP-CL1 was recovered in the TX-insoluble (SDS-soluble) fraction as described above. As shown in Figure 4A, the level of uncleaved GFP-CL1 in cells transfected with A53T was about 30% higher than that in cells transfected with wild-type α-synuclein (Figure 4A, lane 4). A slightly higher level of GFP-CL1 was detected in cells transfected with the A30P mutant (Figure 4A, lane 3) compared with that in cells transfected with wild-type α-synuclein (Figure 4A, lane 2). In contrast, the level of GFP-CL1 in cells transfected with Δ73-83 or β-synuclein was negligible, as was that in control cells (Figure 4A, lane 5 and 6). The expression levels of α-synuclein protein in Tris-soluble fractions were almost the same. These results showed that mutants of α-synuclein that are prone to aggregate *in vitro* have stronger inhibitory effects on cellular proteasome activity than does the wild-type protein and that Δ73-83 and β-synuclein, neither of which form fibrils *in vitro*, do not inhibit the proteasome.

Expression of Phosphomimetic α-Synuclein Mutant S129D Enhanced Its Inhibition of Proteasome Activity. Aggregated α-synuclein in brains of α-synucleinopathy patients

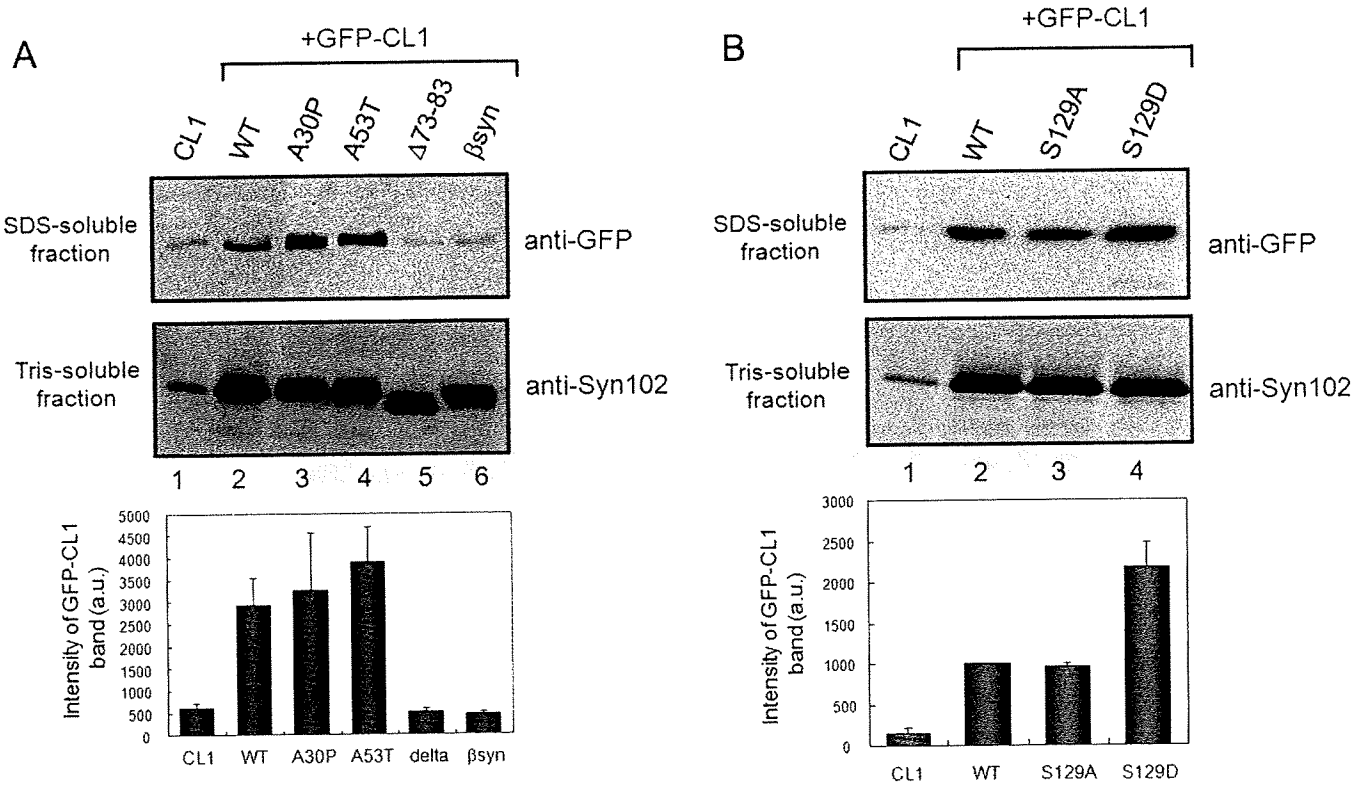

FIGURE 4: Effects of expression of α-synuclein mutants on proteasome activity. (A, B) Immunoblot analyses of extracted proteins from cells transfected with both GFP-CL1 and wild-type α-synuclein or a mutant (A30P, A53T, S129A, S129D, Δ73-83 or β-synuclein). Cells were harvested 72 h after transfection, and Tris-soluble (lower panels) and SDS-soluble fractions (upper panels) were prepared. Immunoblot analyses were performed using anti-GFP (upper panels) or anti-Syn102 (lower panels) antibodies. The results of quantitative analysis of the GFP-CL1 bands, expressed as means + SD (n = 3), are shown below the blot.

is hyperphosphorylated at Ser129, and this post-translational modification facilitates self-aggregation *in vitro* (*3*). Altering Ser129 to the negatively charged residue Asp (S129D) to mimic phosphorylation significantly enhances α-synuclein toxicity in a *Drosophila* model (*34*). We asked whether phosphorylation of α-synuclein might affect proteasome activity in cultured cells. SH-SY5Y cells were transfected with GFP-CL1 and wild-type or mutant α-synuclein. Immunoreactivity of GFP-CL1 in cells transfected with S129A was similar to that of cells transfected with wild-type α-synuclein, while the levels of GFP-CL1 in cells expressing S129D mutant to mimic phosphorylation was significantly higher than those in cells transfected with the wild-type or S129A (Figure 4B). These results suggested that phosphorylation of Ser129 may facilitate inhibition of proteasome function by intracellular α-synuclein.

Comparison of Proteasome Activity Assay Using GFP-CL1 with a Conventional Cleaving Assay Using a Fluorescent Peptide Substrate. To compare the sensitivity of the assay of proteasome activity using GFP-CL1 with that of the conventional assay using a fluorescent peptide, we evaluated biochemically the proteasome activity of lysates from cells transfected with α-synuclein. SH-SY5Y cells were transfected with wild-type α-synuclein for 72 h, and proteasome activity in cell lysates was measured using a peptide substrate specific for proteasome, zLLE-MCA. As shown in Figure 5, zLLE-MCA-cleaving activity in cells transfected with wild-type α-synuclein was decreased slightly (~10% inhibition) compared with that in cells transfected with empty vector, while MG132 had a potent inhibitory effect on proteasome activity (~80% inhibition). On the other hand, as described above, the levels of GFP-CL1 in cells transfected with GFP-CL1 and α-synuclein were increased about

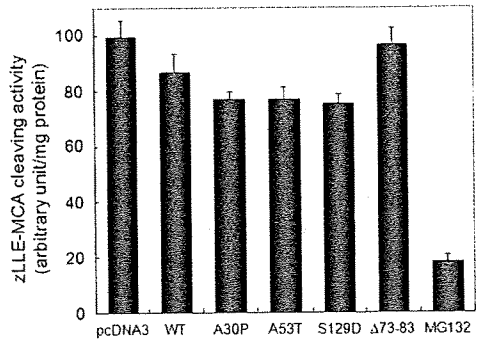

FIGURE 5: Measurements of proteasome activity using a fluorescent peptide substrate. SH-SY5Y cells were transfected with pcDNA3 empty vector, wild-type α-synuclein (WT), A30P, A53T, S129D, Δ73-83 for 72 h or treated with 20 μM MG132 for 6 h. Cytosolic fractions were prepared and assayed using z-LLE-MCA as a substrate. The results were expressed as means + SD (n = 3).

5 times compared with those in cells expressing GFP-CL1 (Figure 4A).

As shown in Figure 5, the zLLE-MCA-cleaving activity in cells transfected with A30P was almost equal to that in cells expressing A53T, which in turn was decreased slightly compared with that in cells transfected with wild-type α-synuclein. Proteasome activity in cells transfected with Δ73-83 was found to be the same as that in cells transfected with empty vector. It was also revealed that S129D had a slightly stronger inhibitory effect on proteasome activity than did wild-type α-synuclein. Taken together, as compared with the results shown in Figure 3 and 4, these results clearly indicate that a method in this study by detecting the fluorescence of GFP-CL1 or immunoblot analysis using

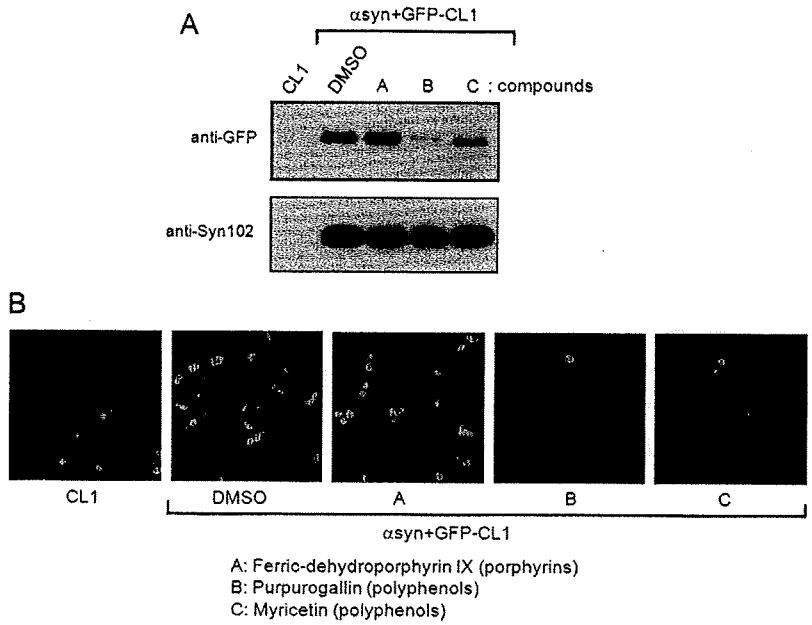

FIGURE 6: Small molecules prevent proteasome dysfunction by intracellular α-synuclein. SH-SY5Y cells were transfected with GFP-CL1 alone or both GFP-CL1 and α-synuclein. Compounds (final 40 μM) were added 2 h after transfection. Cells were harvested after a 72-h incubation and analyzed by immunoblotting (A) and confocal microscopy (B). Immunoblot analyses of Tris-soluble (lower panels) and SDS-soluble fractions (upper panels) were performed using anti-GFP (upper panels) or anti-Syn102 (lower panels) antibodies. The decreased GFP-CL1 level in transfected cells treated with compound B or C, as compared with that of transfected cells treated with vehicle alone (DMSO), indicated that compound B or C, but not compound A, rescued cells from proteasome impairment by expression of α-synuclein.

anti-GFP antibody is a simple and sensitive for monitoring proteasome activity in cells.

Small Molecular Compounds Attenuate Cellular Inhibition of Proteasome Activity by Expression of α-Synuclein. In this study, we have shown that proteasomal activity is impaired by expression of α-synuclein in SH-SY5Y cells. Impairment of proteasome function leads to induction of apoptosis, followed by cell death, so it is important to protect cells from such inhibition by intracellular α-synuclein. These results raised the possibility that our cellular model, in which both GFP-CL1 and α-synuclein are expressed, might be useful to screen for small molecules preventing proteasome inhibition mediated by expression of α-synuclein. Recently, we have reported that several compounds, including polyphenols, phenothiazines, and porphyrins, inhibit aggregation of recombinant α-synuclein *in vitro* (*35*). We therefore asked whether these compounds might affect proteasome inhibition by α-synuclein in cultured cells. Compounds of interest were added to the culture medium of cells transfected with both GFP-CL1 and α-synuclein 2 h after transfection. The cells were incubated for 72 h, harvested and analyzed by immunoblotting and confocal laser microscopy. Immunoblot analyses showed that the level of GFP-CL1 was decreased significantly when cells were treated with purpurogallin or myricetin (polyphenols), but not when they were treated with ferric-dehydroporphyrin IX (porphyrin) (Figure 6A). Cells treated with purpurogallin or myricetin displayed significant decreases in GFP-CL1 fluorescence by confocal microscopy (Figure 6B). Furthermore, we confirmed that exifone and gossypetin, plant polyphenols inhibiting fibril formation of α-synuclein *in vitro* (*35*), also attenuated α-synuclein-mediated proteasome inhibition (data not shown). We further observed that these small molecules did not affect α-synuclein expression (Figure 6A). These results indicate that these compounds may protect cells from proteasome dysfunction arising from expression of α-synuclein.

DISCUSSION

Recent studies have shown that aggregated and monomeric α-synuclein inhibit proteasomal function *in vitro* (*20*, *21*, *36*). In these reports, proteasome activity was measured in a cell-free system using fluorescent peptide substrates, and little is known about the effects of α-synuclein expression on proteasome activity in cultured cells. To examine this question, we tried to establish a sensitive and convenient method to measure proteasome activity using cultured cells transfected with a GFP-CL1 reporter plasmid. We further applied this system to show that transient coexpression of α-synuclein inhibits the proteasome activity of SH-SY5Y cells.

The GFP-CL1 reporter is a useful tool for the detection of proteasome activity in cells (*26*). Recently, Link et al. reported that the expression of GFP-CL1 in *Caenorhabditis elegans* muscle or neurons causes deposition of GFP-CL1 and leads to rapid paralysis (*27*). In this study, we also found that uncleaved GFP-CL1 was largely recovered in TX-insoluble fractions of SH-SY5Y cells transfected with GFP-CL1 and α-synuclein, while α-synuclein was recovered in TS- and TX-soluble fractions (Figure 1B and Figure S1 in Supporting Information), indicating that uncleaved GFP-CL1 was deposited, but α-synuclein was still soluble in transfected cells. Cell death was not detected in either cells transfected with GFP-CL1 alone or cells transfected with both GFP-CL1 and wild-type α-synuclein or mutants thereof, although Link et al. found that GFP-CL1 is toxic when expressed in *C. elegans* muscle cells (*27*). The discrepancy might be due to differences in the cell type used. Further studies are required in this regard. It is surprising that a relatively short addition of 16 residues to the C terminus of GFP can convert this normally soluble protein into a protein that strongly aggregates. We suggest that the C-terminal 16 residues may directly interfere with GFP folding, resulting in misfolded (but still fluorescent) forms that are prone to aggregate.

How does α-synuclein suppress intracellular proteasome activity? Several reports have described that α-synuclein may directly interfere with the proteasome. It was shown that α-synuclein binds to S6′ or S6a, a component of the 19S subunit in the 26S proteasome in cultured cells (*23*, *37*). It was also reported that aggregated α-synuclein, but not its monomer, effectively inhibited the 26S proteasome activity *in vitro* (*20*, *21*, *25*, *36*). Interestingly, we have shown that two pathogenic α-synuclein mutants, A30P and A53T, which are liable to form fibrils or oligomers *in vitro*, inhibited proteasome activity more strongly than did wild-type α-synuclein, while Δ73-83 mutant and β-synuclein, neither of which assemble into filaments *in vitro*, did not inhibit proteasome activity. Although we failed to detect any sarkosyl-insoluble aggregates of α-synuclein in cells transfected with wild-type or mutant α-synuclein (data not shown), these results raise the possibility that soluble prefibrillar intermediates, such as misfolded monomers, oligomers or protofibrils, may inhibit proteasome activity in transfected cells. Additional studies are needed to explore oligomers and protofibrils of α-synuclein in our cell model.

Phosphorylation seems to be a common mechanism controlling the neurotoxicity of aggregation-prone toxic proteins involved in neurodegenerative diseases such as tau (*38*, *39*), α-synuclein (*3*), and TDP-43 (*40*–*42*). We suggested that phosphorylation of α-synuclein may play a role in suppression of proteasome activity in cells. It was reported that expression of S129D mutant α-synuclein in *Drosophila* significantly enhances the toxicity (*34*). However, the mechanisms through which phosphomimetic S129D mutant causes cell death in the fly remain unknown. Phosphorylated α-synuclein at Ser129 is known to be more prone to aggregate than wild-type α-synuclein (*3*), and this may be related to its toxicity. Alternatively, inhibitory effects of the S129D mutant on intracellular proteasome activity, as shown in this study, may be involved in cell death.

Importantly, we have shown that intracellular α-synuclein may be toxic to neuronal cells because the protein causes proteasome dysfunction. It was previously reported that duplication and triplication of α-synuclein gene causes familial PD (*7*–*11*), indicating that overproduction of α-synuclein protein could lead to the onset of PD. It is reasonable to speculate that proteasome activity may also be affected in neurons of these patients in a manner similar to that shown in this study. It may be important to prevent α-synuclein-induced inhibition or decrease of proteasome activity. In this study, we screened for compounds protecting cells from the α-synuclein-mediated proteasome dysfunction and found that purpurogallin, myricetin, exifone, and gossypetin (polyphenols from plants) prevented proteasome impairment by α-synuclein. These compounds are thought to inhibit *in vitro* α-synuclein filament formation by stabilizing soluble prefibrillar intermediates (*35*). We speculate that these small molecules may interact with oligomeric forms of α-synuclein in cultured cells, although we can not exclude the possibility that these compounds directly regulate the activity of the proteasome. The precise mechanisms by which these polyphenols prevent α-synuclein-mediated proteasome dysfunction remain unknown. However, these compounds may be novel drug candidates for neurodegenerative diseases. Our cellular model system using coexpression of GFP-CL1 and α-synuclein should be a sensitive and useful tool for screening of compounds and drugs for the prevention and treatment of these disease.

ACKNOWLEDGMENT

We thank Drs. H. Mimuro and M. Masuda for helpful advice and discussions.

SUPPORTING INFORMATION AVAILABLE

Fractionation of cells expressing both of GFP-CL1 and α-synuclein. This material is available free of charge via the Internet at http://pubs.acs.org.

REFERENCES

1. Spillantini, M. G., Schmidt, M. L., Lee, V. M., Trojanowski, J. Q., Jakes, R., and Goedert, M. (1997) Alpha-synuclein in Lewy bodies. *Nature 388*, 839–840.
2. Baba, M., Nakajo, S., Tu, P. H., Tomita, T., Nakaya, K., Lee, V. M., Trojanowski, J. Q., and Iwatsubo, T. (1998) Aggregation of α-synuclein in Lewy bodies of sporadic Parkinson's disease and dementia with Lewy bodies. *Am. J. Pathol. 152*, 879–884.
3. Fujiwara, H., Hasegawa, M., Dohmae, N., Kawashima, A., Masliah, E., Goldberg, M. S., Shen, J., Takio, K., and Iwatsubo, T. (2002) α-Synuclein is phosphorylated in synucleinopathy lesions. *Nat. Cell Biol. 4*, 160–164.
4. Polymeropoulos, M. H., Lavedan, C., Leroy, E., Ide, S. E., Dehejia, A., Dutra, A., Pike, B., Root, H., Rubenstein, J., Boyer, R., Stenroos, E. S., Chandrasekharappa, S., Athanassiadou, A., Papapetropoulos, T., Johnson, W. G., Lazzarini, A. M., Duvoisin, R. C., Di Iorio, G., Golbe, L. I., and Nussbaum, R. L. (1997) Mutation in the α-synuclein gene identified in families with Parkinson's disease. *Science 276*, 2045–2047.
5. Kruger, R., Kuhn, W., Muller, T., Woitalla, D., Graeber, M., Kosel, S., Przuntek, H., Epplen, J. T., Schols, L., and Riess, O. (1998) Ala30Pro mutation in the gene encoding α-synuclein in Parkinson's disease. *Nat. Genet. 18*, 106–108.
6. Zarranz, J. J., Alegre, J., Gomez-Esteban, J. C., Lezcano, E., Ros, R., Ampuero, I., Vidal, L., Hoenicka, J., Rodriguez, O., Atares, B., Llorens, V., Gomez Tortosa, E., del Ser, T., Munoz, D. G., and de Yebenes, J. G. (2004) The new mutation, E46K, of α-synuclein causes Parkinson and Lewy body dementia. *Ann. Neurol. 55*, 164–173.
7. Singleton, A. B., Farrer, M., Johnson, J., Singleton, A., Hague, S., Kachergus, J., Hulihan, M., Peuralinna, T., Dutra, A., Nussbaum, R., Lincoln, S., Crawley, A., Hanson, M., Maraganore, D., Adler, C., Cookson, M. R., Muenter, M., Baptista, M., Miller, D., Blancato, J., Hardy, J., and Gwinn-Hardy, K. (2003) α-Synuclein locus triplication causes Parkinson's disease. *Science 302*, 841.
8. Chartier-Harlin, M. C., Kachergus, J., Roumier, C., Mouroux, V., Douay, X., Lincoln, S., Levecque, C., Larvor, L., Andrieux, J., Hulihan, M., Waucquier, N., Defebvre, L., Amouyel, P., Farrer, M., and Destee, A. (2004) Alpha-synuclein locus duplication as a cause of familial Parkinson's disease. *Lancet 364*, 1167–1169.
9. Ibanez, P., Bonnet, A. M., Debarges, B., Lohmann, E., Tison, F., Pollak, P., Agid, Y., Durr, A., and Brice, A. (2004) Causal relation between α-synuclein gene duplication and familial Parkinson's disease. *Lancet 364*, 1169–1171.
10. Nishioka, K., Hayashi, S., Farrer, M. J., Singleton, A. B., Yoshino, H., Imai, H., Kitami, T., Sato, K., Kuroda, R., Tomiyama, H., Mizoguchi, K., Murata, M., Toda, T., Imoto, I., Inazawa, J., Mizuno, Y., and Hattori, N. (2006) Clinical heterogeneity of α-synuclein gene duplication in Parkinson's disease. *Ann. Neurol. 59*, 298–309.
11. Ikeuchi, T., Kakita, A., Shiga, A., Kasuga, K., Kaneko, H., Tan, C. F., Idezuka, J., Wakabayashi, K., Onodera, O., Iwatsubo, T., Nishizawa, M., Takahashi, H., and Ishikawa, A. (2008) Patients homozygous and heterozygous for SNCA duplication in a family with parkinsonism and dementia. *Arch. Neurol. 65*, 514–519.
12. Hasegawa, M., Fujiwara, H., Nonaka, T., Wakabayashi, K., Takahashi, H., Lee, V. M., Trojanowski, J. Q., Mann, D., and Iwatsubo, T. (2002) Phosphorylated α-synuclein is ubiquitinated in α-synucleinopathy lesions. *J. Biol. Chem. 277*, 49071–49076.
13. Nonaka, T., Iwatsubo, T., and Hasegawa, M. (2005) Ubiquitination of α-synuclein. *Biochemistry 44*, 361–368.
14. Anderson, J. P., Walker, D. E., Goldstein, J. M., de Laat, R., Banducci, K., Caccavello, R. J., Barbour, R., Huang, J., Kling, K., Lee, M., Diep, L., Keim, P. S., Shen, X., Chataway, T., Schlossmacher, M. G., Seubert, P., Schenk, D., Sinha, S., Gai, W. P., and Chilcote, T. J. (2006) Phosphorylation of Ser-129 is the dominant pathological modification of α-synuclein in familial and sporadic Lewy body disease. *J. Biol. Chem. 281*, 29739–29752.

15. Ciechanover, A., Orian, A., and Schwartz, A. L. (2000) Ubiquitin-mediated proteolysis: biological regulation via destruction. *Bioessays 22*, 442–451.
16. Goldberg, A. L. (2003) Protein degradation and protection against misfolded or damaged proteins. *Nature 426*, 895–899.
17. Tofaris, G. K., Razzaq, A., Ghetti, B., Lilley, K. S., and Spillantini, M. G. (2003) Ubiquitination of α-synuclein in Lewy bodies is a pathological event not associated with impairment of proteasome function. *J. Biol. Chem. 278*, 44405–44411.
18. Sampathu, D. M., Giasson, B. I., Pawlyk, A. C., Trojanowski, J. Q., and Lee, V. M. (2003) Ubiquitination of α-synuclein is not required for formation of pathological inclusions in α-synucleinopathies. *Am. J. Pathol. 163*, 91–100.
19. Liu, C. W., Corboy, M. J., DeMartino, G. N., and Thomas, P. J. (2003) Endoproteolytic activity of the proteasome. *Science 299*, 408–411.
20. Snyder, H., Mensah, K., Theisler, C., Lee, J., Matouschek, A., and Wolozin, B. (2003) Aggregated and monomeric α-synuclein bind to the S6′ proteasomal protein and inhibit proteasomal function. *J. Biol. Chem. 278*, 11753–11759.
21. Lindersson, E., Beedholm, R., Hojrup, P., Moos, T., Gai, W., Hendil, K. B., and Jensen, P. H. (2004) Proteasomal inhibition by α-synuclein filaments and oligomers. *J. Biol. Chem. 279*, 12924–12934.
22. Martin-Clemente, B., Alvarez-Castelao, B., Mayo, I., Sierra, A. B., Diaz, V., Milan, M., Farinas, I., Gomez-Isla, T., Ferrer, I., and Castano, J. G. (2004) α-Synuclein expression levels do not significantly affect proteasome function and expression in mice and stably transfected PC12 cell lines. *J. Biol. Chem. 279*, 52984–52990.
23. Fujita, M., Sugama, S., Nakai, M., Takenouchi, T., Wei, J., Urano, T., Inoue, S., and Hashimoto, M. (2007) α-Synuclein stimulates differentiation of osteosarcoma cells: relevance to down-regulation of proteasome activity. *J. Biol. Chem. 282*, 5736–5748.
24. Stefanis, L., Larsen, K. E., Rideout, H. J., Sulzer, D., and Greene, L. A. (2001) Expression of A53T mutant but not wild-type α-synuclein in PC12 cells induces alterations of the ubiquitin-dependent degradation system, loss of dopamine release, and autophagic cell death. *J. Neurosci. 21*, 9549–9560.
25. Emmanouilidou, E., Stefanis, L., Vekrellis, K. (2008) Cell-produced α-synuclein oligomers are targeted to, and impair, the 26S proteasome, Neurobiol. Aging Epub ahead of print, DOI: 10.1016/j.neurobiolaging.2008.07.008.
26. Bence, N. F., Sampat, R. M., and Kopito, R. R. (2001) Impairment of the ubiquitin-proteasome system by protein aggregation. *Science 292*, 1552–1555.
27. Link, C. D., Fonte, V., Hiester, B., Yerg, J., Ferguson, J., Csontos, S., Silverman, M. A., and Stein, G. H. (2006) Conversion of green fluorescent protein into a toxic, aggregation-prone protein by C-terminal addition of a short peptide. *J. Biol. Chem. 281*, 1808–1816.
28. Tu, P. H., Galvin, J. E., Baba, M., Giasson, B., Tomita, T., Leight, S., Nakajo, S., Iwatsubo, T., Trojanowski, J. Q., and Lee, V. M. (1998) Glial cytoplasmic inclusions in white matter oligodendrocytes of multiple system atrophy brains contain insoluble α-synuclein. *Ann. Neurol. 44*, 415–422.
29. Gilon, T., Chomsky, O., and Kulka, R. G. (1998) Degradation signals for ubiquitin system proteolysis in *Saccharomyces cerevisiae*. *EMBO J. 17*, 2759–2766.
30. David, D. C., Layfield, R., Serpell, L., Narain, Y., Goedert, M., and Spillantini, M. G. (2002) Proteasomal degradation of tau protein. *J. Neurochem. 83*, 176–185.
31. Conway, K. A., Harper, J. D., and Lansbury, P. T. (1998) Accelerated *in vitro* fibril formation by a mutant α-synuclein linked to early-onset Parkinson disease. *Nat. Med. 4*, 1318–1320.
32. Choi, W., Zibaee, S., Jakes, R., Serpell, L. C., Davletov, B., Crowther, R. A., and Goedert, M. (2004) Mutation E46K increases phospholipid binding and assembly into filaments of human α-synuclein. *FEBS Lett. 576*, 363–368.
33. Biere, A. L., Wood, S. J., Wypych, J., Steavenson, S., Jiang, Y., Anafi, D., Jacobsen, F. W., Jarosinski, M. A., Wu, G. M., Louis, J. C., Martin, F., Narhi, L. O., and Citron, M. (2000) Parkinson's disease-associated α-synuclein is more fibrillogenic than β- and γ-synuclein and cannot cross-seed its homologs. *J. Biol. Chem. 275*, 34574–34579.
34. Chen, L., and Feany, M. B. (2005) α-Synuclein phosphorylation controls neurotoxicity and inclusion formation in a *Drosophila* model of Parkinson disease. *Nat. Neurosci. 8*, 657–663.
35. Masuda, M., Suzuki, N., Taniguchi, S., Oikawa, T., Nonaka, T., Iwatsubo, T., Hisanaga, S., Goedert, M., and Hasegawa, M. (2006) Small molecule inhibitors of α-synuclein filament assembly. *Biochemistry 45*, 6085–6094.
36. Snyder, H., Mensah, K., Hsu, C., Hashimoto, M., Surgucheva, I. G., Festoff, B., Surguchov, A., Masliah, E., Matouschek, A., and Wolozin, B. (2005) β-Synuclein reduces proteasomal inhibition by α-synuclein but not γ-synuclein. *J. Biol. Chem. 280*, 7562–7569.
37. Ghee, M., Fournier, A., and Mallet, J. (2000) Rat α-synuclein interacts with Tat binding protein 1, a component of the 26S proteasomal complex. *J Neurochem 75*, 2221–2224.
38. Morishima-Kawashima, M., Hasegawa, M., Takio, K., Suzuki, M., Yoshida, H., Titani, K., and Ihara, Y. (1995) Proline-directed and non-proline-directed phosphorylation of PHF-tau. *J. Biol. Chem. 270*, 823–829.
39. Hasegawa, M., Morishima-Kawashima, M., Takio, K., Suzuki, M., Titani, K., and Ihara, Y. (1992) Protein sequence and mass spectrometric analyses of tau in the Alzheimer's disease brain. *J. Biol. Chem. 267*, 17047–17054.
40. Nonaka, T., Arai, T., Buratti, E., Baralle, F. E., Akiyama, H., and Hasegawa, M. (2009) Phosphorylated and ubiquitinated TDP-43 pathological inclusions in ALS and FTLD-U are recapitulated in SH-SY5Y cells. *FEBS Lett. 583*, 394–400.
41. Inukai, Y., Nonaka, T., Arai, T., Yoshida, M., Hashizume, Y., Beach, T. G., Buratti, E., Baralle, F. E., Akiyama, H., Hisanaga, S., and Hasegawa, M. (2008) Abnormal phosphorylation of Ser409/410 of TDP-43 in FTLD-U and ALS. *FEBS Lett. 582*, 2899–2904.
42. Hasegawa, M., Arai, T., Nonaka, T., Kametani, F., Yoshida, M., Hashizume, Y., Beach, T. G., Buratti, E., Baralle, F., Morita, M., Nakano, I., Oda, T., Tsuchiya, K., and Akiyama, H. (2008) Phosphorylated TDP-43 in frontotemporal lobar degeneration and amyotrophic lateral sclerosis. *Ann. Neurol. 64*, 60–70.

THE JOURNAL OF BIOLOGICAL CHEMISTRY VOL. 284, NO. 25, pp. 16840–16847, June 19, 2009

Effect of Pin1 or Microtubule Binding on Dephosphorylation of FTDP-17 Mutant Tau*[S]

Received for publication, April 2, 2009, and in revised form, April 25, 2009 Published, JBC Papers in Press, April 28, 2009, DOI 10.1074/jbc.M109.003277

Kensuke Yotsumoto[‡1], Taro Saito[‡1], Akiko Asada[‡], Takayuki Oikawa[‡§], Taeko Kimura[‡], Chiyoko Uchida[¶], Koichi Ishiguro[‖], Takafumi Uchida[**], Masato Hasegawa[§], and Shin-ichi Hisanaga[‡2]

From the [‡]Department of Biological Sciences, Faculty of Science and Engineering, Tokyo Metropolitan University, 1-1 Minami-osawa, Hachioji, Tokyo 192-0397, the [§]Laboratory of Molecular Neurobiology, Tokyo Metropolitan Institute of Psychiatry, Kamikitazawa, Setagaya, Tokyo 156-8585, the [¶]University Health Center, Ibaraki University, Mito, Ibaraki 310-8512, the [‖]Mitsubishi Kagaku Institute of Life Science, Machida, Tokyo 194-8511, and the [**]Department of Molecular Cell Biology, Graduate School of Agricultural Science, Tohoku University, Sendai, Miyagi 981-8555, Japan

Neurodegenerative tauopathies, including Alzheimer disease, are characterized by abnormal hyperphosphorylation of the microtubule-associated protein Tau. One group of tauopathies, known as frontotemporal dementia with parkinsonism linked to chromosome 17 (FTDP-17), is directly associated with mutations of the gene *tau*. However, it is unknown why mutant Tau is highly phosphorylated in the patient brain. In contrast to *in vivo* high phosphorylation, FTDP-17 Tau is phosphorylated less than wild-type Tau *in vitro*. Because phosphorylation is a balance between kinase and phosphatase activities, we investigated dephosphorylation of mutant Tau proteins, P301L and R406W. Tau phosphorylated by Cdk5-p25 was dephosphorylated by protein phosphatases in rat brain extracts. Compared with wild-type Tau, R406W was dephosphorylated faster and P301L slower. The two-dimensional phosphopeptide map analysis suggested that faster dephosphorylation of R406W was due to a lack of phosphorylation at Ser-404, which is relatively resistant to dephosphorylation. We studied the effect of the peptidyl-prolyl isomerase Pin1 or microtubule binding on dephosphorylation of wild-type Tau, P301L, and R406W *in vitro*. Pin1 catalyzes the *cis/trans* isomerization of phospho-Ser/Thr-Pro sequences in a subset of proteins. Dephosphorylation of wild-type Tau was reduced in brain extracts of Pin1-knockout mice, and this reduction was not observed with P301L and R406W. On the other hand, binding to microtubules almost abolished dephosphorylation of wild-type and mutant Tau proteins. These results demonstrate that mutation of Tau and its association with microtubules may change the conformation of Tau, thereby suppressing dephosphorylation and potentially contributing to the etiology of tauopathies.

One of hallmarks of Alzheimer disease (AD)[3] pathology is neurofibrillary tangles, which are composed of paired helical filaments (PHFs), aggregates of the abnormally phosphorylated microtubule-associated protein Tau. Intracellular inclusions comprising Tau are also found in several other neurodegenerative diseases, including Pick disease, progressive supranuclear palsy, corticobasal degeneration, and frontotemporal dementia with parkinsonism linked to chromosome 17 (FTDP-17), collectively called tauopathies (1–3). Identification of Tau as a causative gene of the inherited tauopathy FTDP-17 reveals that Tau mutation is sufficient to cause disease (4–6). However, the impact Tau mutations have on neurodegeneration remains unknown.

Tau proteins in inclusions are hyperphosphorylated, and extensive studies have identified the phosphorylation sites; for example, more than 20 sites have been identified in PHF-Tau obtained from AD brains (7, 8). Tau can be phosphorylated by a variety of protein kinases, including glycogen synthase kinase 3β (GSK3β), cyclin-dependent kinase 5 (Cdk5), mitogen-activated protein kinase, cAMP-dependent protein kinase (PKA), microtubule affinity regulating kinase, and others (9–11). Tau is predominantly phosphorylated on the Ser or Thr residue in Ser/Thr-Pro sequences, suggesting the involvement of proline-directed protein kinases such as GSK3β and Cdk5 in hyperphosphorylation. A critical question is how mutations in Tau induce hyperphosphorylation in brain (12). Early phosphorylation experiments *in vitro* and in cultured cells have shown that mutant Tau is less phosphorylated than wild-type (WT) Tau (13–18). However, two later studies demonstrated higher phosphorylation of mutant Tau using brain extracts as a source of protein kinases in the presence of protein phosphatase inhibitor okadaic acid (19) or in immortalized cortical cells (20). However, it is not fully understood how mutant Tau becomes highly phosphorylated *in vivo*.

Tau hyperphosphorylation could also be attributed to reduced dephosphorylation activity. Tau is dephosphorylated *in vitro* by any of the major four classes of protein phosphatases, PP1, PP2A, PP2B, and PP2C, but PP2A is thought to be the major protein phosphatase that regulates Tau phosphorylation state in brains (21–23). PP2A activity reportedly is decreased in AD brain (24–26), and highly phosphorylated Tau in PHF is

* This work was supported in part by grants-in-aid for scientific research on Priority Area from MEXT of Japan (to S. H.).

[S] The on-line version of this article (available at http://www.jbc.org) contains supplemental Figs. S1–S4.

[1] Both authors contributed equally to this work.

[2] To whom correspondence should be addressed: Tokyo Metropolitan University at 1-1 Minami-osawa, Hachioji, Tokyo 192-0397, Japan. Tel.: 81-42-677-2769; Fax: 81-42-677-2559; E-mail: hisanaga-shinichi@tmu.ac.jp.

[3] The abbreviations used are: AD, Alzheimer disease; Cdk5, cyclin-dependent kinase 5; FTDP-17, frontotemporal dementia with parkinsonism linked to chromosome 17; GSK3β, glycogen synthase kinase 3β; MT, microtubule; PHF, paired helical filament; PKA, cAMP-dependent protein kinase; PP1, protein phosphatase 1; PP2A, protein phosphatase 2A; MOPS, 4-morpholinepropanesulfonic acid; WT, wild type.

relatively resistant to dephosphorylation by PP2A (27). Few studies have been done on dephosphorylation of mutant Tau, however, and thus the mechanism remains unclear. One putative factor involved in mutant Tau dephosphorylation is the peptidyl-prolyl isomerase Pin1. Pin1 catalyzes the *cis/trans* isomerization of phospho-Ser/Thr-Pro sequences in a subset of proteins (28, 29). Pin1 is involved in AD pathogenesis as shown by the fact that it is found in neurofibrillary tangles and that Tau is hyperphosphorylated in Pin1-deficient mouse brains (30). Pin1 is indicated to facilitate Tau dephosphorylation via PP2A by binding to the phospho-Thr-231-Pro or phospho-Thr-212-Pro site (31–33). The effect of Pin1 on the stability of mutant Tau was recently reported (34), but a detailed analysis of Pin1 action on mutant Tau has not been reported. Another possible factor affecting dephosphorylation of mutant Tau is the binding to microtubules. We previously showed that phosphorylation of Tau is stimulated upon binding to microtubules (35). We thus hypothesized that binding to microtubules may also affect the extent of Tau dephosphorylation.

Here, we examined the effects of Pin1 and binding to microtubules on dephosphorylation of WT and FTDP-17 mutant (P301L and R406W) Tau proteins that had been phosphorylated by Cdk5-p25 or Cdk5-p35. P301L and R406W are two distinct types of FTDP-17 mutants that have been studied well. We show for the first time how the regulation of Tau dephosphorylation can contribute to the observed Tau hyperphosphorylation in tauopathies.

EXPERIMENTAL PROCEDURES

Enzymes, Plasmids, and Chemicals—The catalytic subunit of each of PP1 and PP2A was purchased from Upstate (Lake Placid, NY). Brain extract of Pin1-knockout mice and the preparation of GST-Pin1 have been described (36). Cdk5/p35 and Cdk5/p25 were prepared from Sf9 cells as described (37). GSK3β and the catalytic subunit of PKA were purified from rat brain extract as described (38). GSK3β purchased from Millipore (Billerica, MA) was also used for some experiments.

Expression and Purification of Recombinant Human Tau—cDNAs encoding recombinant human WT and FTDP-17 mutant Tau (P301L and R406W, respectively) with one N-terminal insert and four repeat domains (1N4R, see supplemental Fig. S4*A*) in the pRK172 bacterial expression vector were used to transform *Escherichia coli* BL21(DE3)-competent cells (35, 39). ΔMTB, Tau without microtubule-binding repeats, was constructed by PCR with primers 5′-AATAAAAAGATTGAAACCCACAAGCTGAC-3′ (sense) and 5′-ATTCTTCAGGTCTGGCATGG-3′ (antisense). The PCR product was phosphorylated by T4 polynucleotide kinase and ligated into pSG5. The accuracy of the construct was verified by DNA sequencing. Tau proteins were purified from the heat-stable supernatant of the *E. coli* extract by chromatography on a Mono S column as described (35).

Preparation of Tubulin and Binding of Tau to Microtubules—Tubulin was prepared from porcine brains by three cycles of temperature-dependent polymerization/depolymerization (40). Tubulin was separated from microtubule-associated proteins using a phosphocellulose column (P11, Whatman, Brentford, UK) as described (40). Tau (0.05 mg/ml) was bound to microtubules, which were polymerized from 0.5 mg/ml tubulin with an aid of 20 μM taxol in 20 mM MOPS, pH 6.8, and 1 mM $MgCl_2$ by incubation at 35 °C for 20 min as described (35).

Preparation of Phosphorylated Tau (P-Tau)—Recombinant Tau (0.1 mg/ml) was phosphorylated with Cdk5-p35 or Cdk5-p25 in 20 mM MOPS, pH 6.8, and 1 mM $MgCl_2$, in the presence of 0.1 mM [γ-^{32}P]ATP for 1 h at 35 °C. Excess [γ-^{32}P]ATP was removed by gel-filtration on a Sephadex G-50 column. Fractions containing P-Tau were pooled, stored at −80 °C, and used for dephosphorylation experiments within 10 days.

Dephosphorylation of P-Tau—P-Tau (0.05 mg/ml) was incubated with rat brain extracts at 35 °C for various times in 20 mM HEPES, pH 7.4, 1 mM $MgCl_2$ and 1 mM EDTA. Dephosphorylation was stopped by addition of 4× SDS-PAGE sample buffer. After boiling for 2 min, the samples were subjected to SDS-PAGE. The remaining ^{32}P-Tau was estimated by a FLA-7000 Bioimage Analyzer (Fujifilm, Tokyo, Japan). Dephosphorylation was defined as the amount of phosphate removed from P-Tau during incubation. Dephosphorylation of experimental samples was expressed as a percentage of that of P-WT Tau by WT rat or mouse brain extracts.

Two-dimensional Phosphopeptide Microtubule-associated Protein Analysis—P-Tau separated by SDS-PAGE was digested in gel slices by trypsin (Sigma) in 50 mM NH_4HCO_3, pH 8.4, at 30 °C overnight. The resulting tryptic peptides were subjected to two-dimensional phosphopeptide mapping using a thin-layer cellulose plate (catalogue number 1.05716.0001, Merck, Darmstadt, Germany) (35). Electrophoresis was performed at pH 1.9, and ascending chromatography was performed in *n*-butyl alcohol/pyridine/glacial acetic acid/water (150/100/30/120). Phosphopeptide spots were detected, and the intensity was measured by a FLA-7000 Bioimage Analyzer.

RESULTS

Dephosphorylation of FTDP-17 Mutant Tau, P301L, and R406W—Purified, recombinant Tau, either WT Tau or FDTP-17 mutant Tau P301L or R406W, was phosphorylated *in vitro* by Cdk5-p25 in the presence of [γ-^{32}P]ATP (supplemental Fig. S1*A*). About 4 mol of phosphate was incorporated into 1 mol of WT Tau. ^{32}P bound to WT Tau was easily removed by incubation with brain extract (*BE*) but not without the brain extract (−) (Fig. 1*A*). The Tau protein was not degraded during incubation. The decrease in the ^{32}P label on Tau was inhibited by the protein phosphatase inhibitor, microcystin LR (supplemental Fig. S2*A*), indicating that the decrease in the ^{32}P label is dephosphorylation. We measured the dephosphorylation of *in vitro* phosphorylated P301L and R406W; P-P301L was dephosphorylated slower and P-R406W faster than P-WT Tau (Fig. 1*B*). These results constitute the evidence of differential rates of dephosphorylation between WT and mutant Taus.

Tau is mainly dephosphorylated by PP2A (21–23, 25). To determine whether our observed difference in dephosphorylation (Fig. 1*B*) was due to PP2A activity, we dephosphorylated P-Tau by rat brain extract in the presence of phosphatase inhibitor. Dephosphorylation was inhibited by okadaic acid at 10 nM, the concentration specific to PP2A, but not inhibited by inhibitor-2 (40 nM), a heat-stable inhibitory protein for PP1 (Fig. 1*C*). We confirmed the results using the purified catalytic subunit of

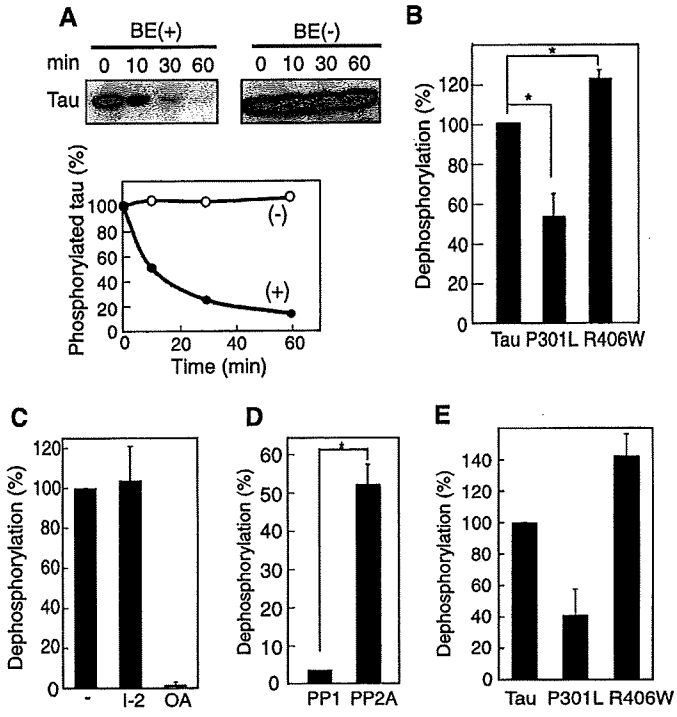

FIGURE 1. **Dephosphorylation of phosphorylated WT and mutant Tau by rat brain extract.** *A*, purified recombinant WT Tau phosphorylated by Cdk5/p25 in the presence of [γ-^{32}P]ATP was incubated without (−) or with rat brain extract (*BE*) for the indicated times. After the samples were subjected to SDS-PAGE, radioactivity associated with Tau was detected by a FLA-7000 Bioimage Analyzer (*upper panels*) and quantified (*lower panel*). *B*, dephosphorylation of P-WT Tau, P-P301L, and P-R406W by rat brain extract. Dephosphorylation was defined as the signals removed from P-Tau during a 10-min incubation, and the respective dephosphorylation is expressed as the percentage relative to that measured for WT Tau. *C*, dephosphorylation of P-WT Tau by rat brain extract in the presence of 40 nM inhibitor-2 or 10 nM okadaic acid. *D*, dephosphorylation of P-WT Tau by the catalytic subunit of PP1 or PP2A (0.1 unit/ml for each). *E*, dephosphorylation of P-WT Tau, P-P301L, or P-R406W by PP2A.

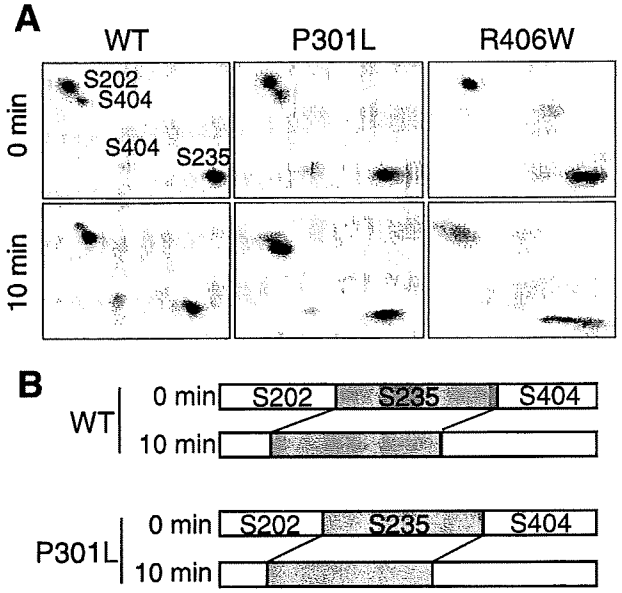

FIGURE 2. **Phosphorylation site-dependent dephosphorylation of Tau.** *A*, two-dimensional phosphopeptide maps of phosphorylated WT, P301L, and R406W Tau before (0 min) and after a 10-min incubation with the rat brain extract. The radioactivity applied to cellulose plates was adjusted to 1000 cpm. The quantification of the respective spots in P-WT Tau and P-P301L is shown in (*B*). The relative signal intensity of the Ser-202, Ser-235, and Ser-404 phosphorylation sites is expressed as a fraction of the total signals of these phosphorylation spots in WT and P301L before (0 min) and after (10 min) dephosphorylation. These data are representative of those obtained from three different experiments.

PP1 or PP2A. P-Tau was dephosphorylated by PP2A much faster than by PP1 (Fig. 1*D*), consistent with previous reports (22, 25). Further, P-P301L was dephosphorylated by PP2A slower and P-R406W faster compared with P-WT Tau (Fig. 1*E*), as observed in the brain extract experiments (Fig. 1*B*). These data suggest that PP2A is the major protein phosphatase differentially dephosphorylating these Tau substrates (*i.e.* FTDP-17 mutants and WT Tau) in brain extract.

Difference in Dephosphorylation Rate among Phosphorylation Sites on Tau—WT and P301L Tau are phosphorylated mainly at Ser-202, Ser-235, and Ser-404 by Cdk5-p25, and R406W is phosphorylated mainly at Ser-202 and Ser-235 (35). We analyzed the dephosphorylation rate at these sites in P301L or R406W by two-dimensional phosphopeptide mapping. Indeed, Ser-202, Ser-235, and Ser-404 were phosphorylated in WT Tau and P301L, and Ser-202 and Ser-235 in R406W (Fig. 2*A*, 0 min), as shown previously (35). Two-dimensional phosphopeptide patterns after 10 min of dephosphorylation in the brain extract were similar to those before incubation, although there were differences in relative intensity (Fig. 2*A*). We quantified the phosphorylation signals in each of four spots in WT or P301L and expressed them as a fraction of the sum of these four phosphorylation spots (Fig. 2*B*). The data clearly show that Ser-202 was dephosphorylated faster than Ser-404. Because R406W lacks Ser-404 phosphorylation, these also results suggest a rationale for why R406W is dephosphorylated faster than WT or P301L.

Effect of Pin1 on Dephosphorylation of FTDP-17 Mutant Tau Proteins—The prolyl-peptidyl isomerase Pin1 facilitates PP2A-dependent dephosphorylation of P-Tau by converting the *cis* peptide bond of proline at phospho-Ser/Thr-Pro sites to the *trans* conformation (31), thereby yielding a more kinetically favorable P-Tau substrate. However, its effect on dephosphorylation of mutant Tau has not been examined. We measured dephosphorylation of P-WT Tau and P-mutant Taus in brain extracts from Pin1-KO and WT mice. An incubation time of 10 min was chosen as the optimum condition for detecting the difference (supplemental Fig. S2*B*). Dephosphorylation of P-Tau was slower in Pin1-KO mouse brain extract compared with WT mouse brain extract (Fig. 3*A* and *B*), and the dephosphorylation rate increased upon addition of purified Pin1 at 2 nM (Fig. 3*B*, *WT*), a concentration that is sufficient to restore the dephosphorylation activity in Pin1-KO mice (41). This result is consistent with the report that Pin1 enhances dephosphorylation of P-Tau by PP2A (32). We then compared dephosphorylation of P-P301L and P-R406W in Pin1-KO and WT extracts. Interestingly, there was less of a difference in dephosphorylation between Pin1-KO and WT mouse brain extract in P301L and R406W compared with WT Tau; moreover, addition of purified Pin1 to Pin1-KO mouse brain extract did not stimulate the dephosphorylation rate of P-P301L and P-R406W (Fig. 3*B*). These results suggest that FTDP-17 mutations confer insensitivity of P-Tau to Pin1-dependent enhancement of dephosphorylation.

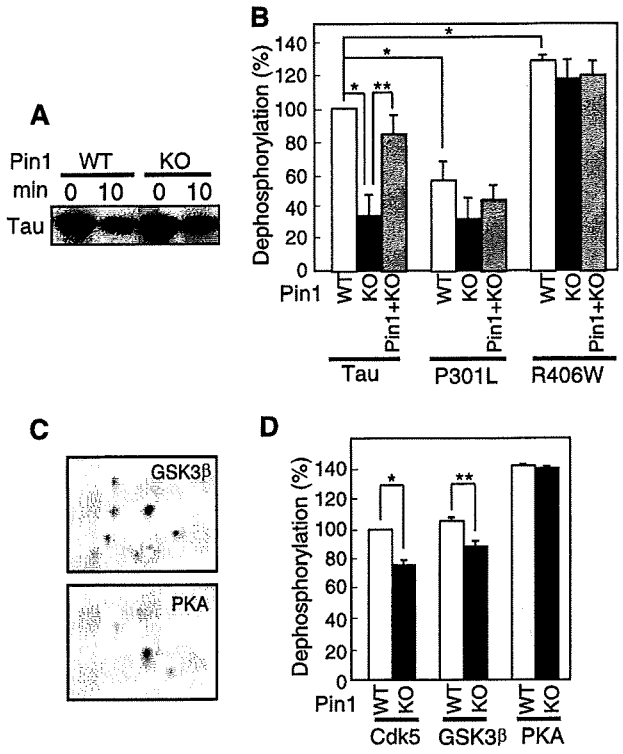

FIGURE 3. **Effect of Pin1 on dephosphorylation of P-WT tau and P-mutant Tau proteins.** *A*, autoradiogram of Tau dephosphorylated in Pin1-KO or WT mouse brain extract for 10 min. *B*, dephosphorylation of P-WT Tau, P-P301L, and P-R406W by brain extract from WT or Pin1-KO mice, or Pin1-KO mouse brain extract supplemented with purified Pin1. *C*, two-dimensional phosphopeptide maps of Tau phosphorylated by GSK3β or PKA. *D*, dephosphorylation of WT Tau phosphorylated with Cdk5/p25, GSK3β, or PKA by brain extract from Pin1-KO or WT mice. Dephosphorylation is expressed as the percentage of the dephosphorylation of P-WT Tau by WT mouse brain extract.

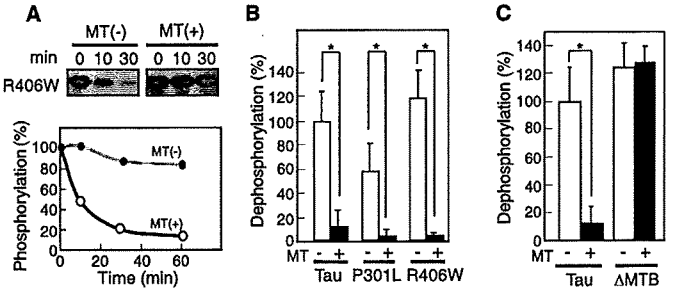

FIGURE 4. **Dephosphorylation of P-Tau bound to microtubules.** *A*, autoradiogram showing ^{32}P-labeled phosphate remaining on R406W Tau incubated with rat brain extract for 10 or 30 min in the absence (−) or presence (+) of microtubules (*MT*). The radioactivity was quantified and is presented graphically in the *lower panel*. *B*, dephosphorylation of P-WT Tau, P-P301L, or P-R406 by rat brain extract in the absence (−) or presence (+) of microtubules (*MT*). *C*, dephosphorylation of P-WT Tau or P-ΔMTB by rat brain extract in the absence (−) or presence (+) of microtubules (*MT*). Dephosphorylation is expressed as the percentage of the dephosphorylation of WT Tau by rat brain extract. *p* values were calculated using Student's *t* test and the *bars* indicate the means ± S.E. of three experiments; *, $p < 0.01$.

We next addressed whether the effect of Pin1 deficiency on dephosphorylation was specific for the phospho-Ser/Thr-Pro sequence. For this experiment, in addition to using Cdk5 we used two other protein kinases, GSK3β, a proline-directed kinase, and PKA, a non-proline-directed kinase, to phosphorylate Tau. About 2–3 mol of phosphate was incorporated into Tau after incubation with these protein kinases (supplemental Fig. S1*B*), but two-dimensional phosphopeptide maps were different between them as expected based on their different phosphorylation sites (Fig. 3*C*). Respective phosphopeptide maps are similar to those of GSK3β- and PKA-phosphorylated Tau reported previously (42). P-WT Tau phosphorylated by GSK3β or PKA was dephosphorylated easily by WT brain extract (Fig. 3*D*). The dephosphorylation of GSK3β-phosphorylated WT Tau as well as Cdk5-phosphorylated WT Tau was decreased in the presence of Pin1-KO mouse brain extract, but this was not the case for PKA-phosphorylated WT Tau, consistent with previous results that the effect of Pin1 on dephosphorylation is specific for certain phosphorylation sequences (31–33).

Dephosphorylation of P-Tau Bound to Microtubules—Phosphorylation of Tau is stimulated when Tau is bound on microtubules (40). Further, phosphorylation by Cdk5-p35 or Cdk5-p25 of mutant Tau bound to microtubules is enhanced to the same extent as that of WT Tau (35). We thus hypothesized that binding to microtubules may also affect dephosphorylation of Tau. WT Tau, P301L, or R406W (0.05 mg/ml), each of which had been phosphorylated by Cdk5-p25, was bound to taxol-polymerized microtubules. Under our experimental conditions, essentially 100% of P-Tau was bound to microtubules. When microtubule-bound P-R406W was incubated with rat brain extract, dephosphorylation was almost completely abolished, whereas unbound P-R406W was quickly dephosphorylated (Fig. 4*A*). Similar results were obtained for P-WT Tau and P-P301L (Fig. 4*B*).

Several control experiments were performed to substantiate the above results. First, we verified that the tubulin fraction did not contain protein kinases, which could counter any dephosphorylation. In this regard, we checked the phosphorylation state of P-WT Tau after incubation with microtubules; no change was evident, indicating that the tubulin fraction contained neither Tau kinases nor phosphatases (supplemental Fig. S3*A*). Second, we verified that the GTP used for tubulin polymerization did not act as a competitive substrate for dephosphorylation; we found that dephosphorylation proceeded at a similar rate in the absence or presence of 0.5 mM GTP (supplemental Fig. S3*B*). Third, we verified that tubulin did not inhibit the protein phosphatases in brain extract. To test this possibility, we used an alternate substrate, neurofilament light chain (NF-L, in this case phosphorylated by Cdk5-p25), which does not interact with microtubules (38). Dephosphorylation of NF-L proceeded in the presence of microtubules, indicating that tubulin does not inhibit brain extract phosphatases (supplemental Fig. S3*C*). Fourth, it has been suggested that the repeat region of Tau binds to the interior of microtubules when tubulin is co-assembled with Tau (43), and thus we verified that P-WT Tau did not bind inside of microtubules in our system. We added P-WT Tau to pre-assembled microtubules and measured dephosphorylation. Indeed, the order of P-WT Tau addition did not affect its dephosphorylation (supplemental Fig. S3*D*).

The above results suggested that, upon binding to microtubules, P-Tau changes its conformation such that dephosphorylation is unfavorable. To demonstrate this possibility more clearly, we used a mutant Tau, ΔMTB, in which the microtubule-binding domain (residues 256–367 according to the long-

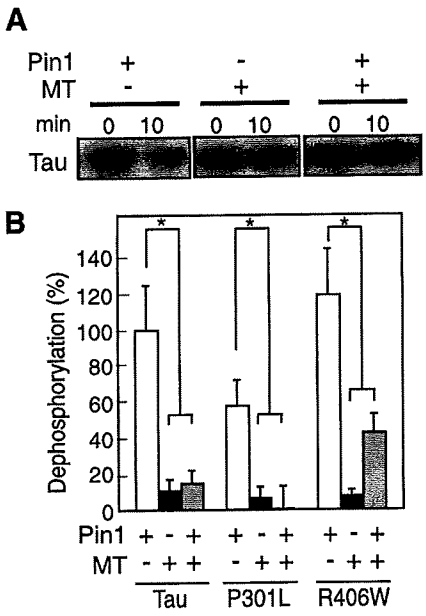

FIGURE 5. **Effect of Pin1 on dephosphorylation of P-Tau in the absence or presence microtubules.** *A*, autoradiograms of P-WT Tau on microtubules (*MT*) incubated with Pin1-KO mouse brain extract supplemented with 2 μM purified Pin1 (+, *lanes 5* and *6*) or not (−, *lanes 3* and *4*) for 0 or 10 min. Dephosphorylation of free P-WT Tau is shown in *lanes 1* and *2*. *B*, dephosphorylation of P-WT Tau, P-P301L, or P-R406W in the absence (−) or presence (+) of microtubules (*MT*) by Pin1-KO mouse brain extract supplemented with Pin1 (+) or not (−). Dephosphorylation of free Tau is shown in the *left bar* of each set of data. Dephosphorylation is expressed as the percentage of the extent of WT Tau dephosphorylation by Pin1-KO mouse brain extract in the absence of microtubules (*MT*). *p* values were calculated using Student's *t* test, and the bars indicate the means ± S.E. of three experiments; *, $p < 0.01$.

est human Tau 441) was deleted (supplemental Fig. S4*A*). ΔMTB did not bind to microtubules effectively (supplemental Fig. S4*B*), as shown previously (44), but it was phosphorylated at the same sites as WT Tau, as demonstrated by two-dimensional phosphopeptide mapping (supplemental Fig. S4*C*). P-ΔMTB Tau and P-WT Tau were dephosphorylated at similar rates when incubated with WT mouse brain extract (Fig. 4*C*); however, dephosphorylation of P-ΔMTB was not suppressed in the presence of microtubules. Taken together, these results indicate that the binding of P-Tau to microtubules suppresses its dephosphorylation.

Effect of Pin1 on Dephosphorylation of P-Tau Bound to Microtubules—We examined the effect of exogenously added Pin1 on dephosphorylation of P-WT Tau bound to microtubules. Addition of purified Pin1 to Pin1-KO mouse brain extract did not enhance the dephosphorylation of P-WT Tau bound to microtubules (compare *lane 6* with *lane 4* in Fig. 5*A*). Dephosphorylated in the absence of microtubules is shown in *lane 2* of Fig. 5*A*. Similar results were obtained with P301L and R406W (Fig. 5*B*). Although Pin1 appeared to increase the dephosphorylation of R406W, the increase was not statistically significant. Thus, Pin1 could not eliminate the suppression of P-Tau dephosphorylation upon microtubule binding.

DISCUSSION

We investigated dephosphorylation of P-Taus, namely WT, P301L, and R406W, phosphorylated by Cdk5-p25. Compared with P-WT Tau, P-R406W was dephosphorylated faster and P-P301L slower. The dephosphorylation rate differed between phosphorylation sites; Ser-404 was dephosphorylated slower and Ser-202 was faster than Ser-235. The latter could explain why P-R406W, which lacks Ser-404 phosphorylation, was dephosphorylated faster than P-WT Tau or P-P301L. We confirmed that dephosphorylation of Tau was attenuated in mouse brain extract lacking Pin1. Of import is that the Pin1 deficiency was countered by the FTDP-17 mutation of Tau. Furthermore, dephosphorylation of P-Tau, either WT or mutants, was almost completely abolished upon binding to microtubules. These findings demonstrate that the phosphorylation states of Tau are actively regulated not only by activation of protein kinases but also by dephosphorylation reactions that depend presumably on the conformational state(s) of Tau under normal or pathologic conditions.

Hyperphosphorylation is a characteristic of Tau in tauopathic brains (11, 12, 45). However, it is not known how FTDP-17 mutations induce hyperphosphorylation. There was a discrepancy between *in vivo* and *in vitro* phosphorylation status of FTDP-17 Tau (13–16, 45). Two recent reports describe higher phosphorylation of mutant Tau (19, 20), but the molecular mechanism that induces abnormal phosphorylation of mutant Tau remains to be elucidated. Because phosphorylation is a balance between kinase and phosphatase activities, we addressed this issue with respect to dephosphorylation, which for FTDP-17 mutant Taus has not been thoroughly examined. We chose P301L and R406W because they represent two distinct types of FTDP-17 mutation that often have been compared. The early-onset mutation, P301L, is one of the most frequently identified mutations in FTDP-17 and has severe phenotypes (6, 46, 47). By contrast, R406W is late onset and has mild phenotypes (4, 48). These mutations differ in fibrillar formation: P301L can selectively form filaments on its own (45, 49), whereas R406W forms filaments by assembling with WT Tau (45, 50). *In vitro* studies have demonstrated that both P301L and R406W mutations reduce the ability of Tau to promote microtubule assembly (39, 51), whereas the effect of R406W on microtubules dynamics is comparable to that of WT Tau in cells (52). Here, a difference in dephosphorylation rate was also found between P301L and R406W. P301L was dephosphorylated slower than WT Tau, and R406W was dephosphorylated faster than WT Tau. Very recently, the effect of FTDP-17 mutations on site-specific dephosphorylation was reported using HEK-293 cell extract as a source of protein phosphatases (53). Considering that most FTDP-17 mutants have properties similar to P301L rather than R406W, reduced dephosphorylation of P301L may account, at least in part, for the observed high levels of phosphorylation of mutant Tau in brains afflicted with tauopathies.

Although both P301L and R406W are highly phosphorylated *in vivo*, their rate of dephosphorylation differed *in vitro*. Under our *in vitro* phosphorylation conditions, Cdk5/p25 mainly phosphorylated Ser-202, Ser-235, and Ser-404 in P301L as well as WT Tau. Among these serines, Ser-202 was dephosphorylated faster and Ser-404 was dephosphorylated slower by protein phosphatases in brain extract. The resistance of Ser-404 to dephosphorylation was recently reported (54). Unlike P301L, R406W is not phosphorylated on Ser-404. The lack of Ser-404

phosphorylation in the R406W mutant also has been reported in R406W-overexpressing mouse brain (15, 17, 55). Mutation of Arg-406 in the Ser-Pro-Arg sequence to Trp may disrupt Cdk5 recognition of the phosphorylation site. Clearly, the absence of phosphorylation at a site that is dephosphorylated slower in other Taus results in the apparent faster dephosphorylation of R406W. However, the phosphorylation in the C-terminal tail region involving Ser-396, Ser-400, and Ser-404 is complex. Phosphorylation at Ser-404 affects any subsequent phosphorylation at Ser-400 and then Ser-396 in a hierarchical manner (56). In contrast, it also has been reported that Ser-396 phosphorylation is elevated in R406W when phosphorylated *in vitro* by brain extract in the presence of okadaic acid (19). It may be interesting to quantify the relative phosphorylation state and dephosphorylation rate of Ser-400 and Ser-396 in R406W, because phosphorylation at Ser-396 and Ser-404 is well known as the PHF1 epitope, one of the abnormal phosphorylation sites in PHF Tau (57).

The site-dependent difference in dephosphorylation rate does not underlie the observed high phosphorylation of mutant Taus, because P301L shares the same phosphorylation pattern as WT Tau. We do not know the answer to explain the issue at present. But the number of microtubule-binding repeats in Tau may be involved in this question. The P301L mutation is located in the C-terminal side of the second microtubule-binding repeat that is found only in four-repeat Tau. This mutation is shown to change the local conformation to increase the propensity of the β-sheet around it, from Lys-298 to Gly-305 (58). This subtle change may increase the interaction of basic amino acids in the repeats, which are the tubulin interacting residues, with phosphorylation sites in the flanking regions. This may result in reduced accessibility by protein phosphatases.

We examined whether Pin1 could distinguish between mutant and WT Taus, because Pin1 facilitates the dephosphorylation of the phospho-Ser/Thr-Pro sequence by PP2A (31). Further, Pin1 dysfunction is indicated in AD pathogenesis, because the protein is detected in neurofibrillary tangles, and Tau is hyperphosphorylated in Pin1-deficient mouse brains (30). We confirmed here that Pin1 enhances dephosphorylation of P-Tau by PP2A, and this enhanced dephosphorylation occurred at proline-directed phosphorylation sites. More important was loss of the Pin1-sensitive enhancement of dephosphorylation in both P301L and R406W. These results predict that P301L and R406W would be phosphorylated more extensively in Pin1 KO mouse brain. We cannot explain why the dephosphorylation of FTDP-17 mutants was insensitive to Pin1, but both P-P301L and P-R406W may have a conformation that cannot be recognized by Pin1. Pin1 binding sites in Tau are reported to be phospho-Thr-231-Pro (30) or phospho-Thr-212-Pro (32, 59). Cdk5 phosphorylation sites at Ser-202, Ser-235 and Ser-404, however, are not included in these Pin1 binding sites. Thus, there may be unidentified Pin1 binding sites among Cdk5-specific phosphorylation sites. It was recently reported that Pin1 differentially affects the *in vivo* half-life of P301L and R406W; P301L is destabilized by Pin1 deficiency, whereas R406W and WT Tau are stabilized (34). It would be interesting to examine any relationship between Pin1-dependent dephosphorylation of Taus and their stability.

Binding to microtubules remarkably affects dephosphorylation of Tau. In general our results agree with those of Sontag *et al.* (60) that dephosphorylation of PKA-phosphorylated Tau by purified PP2A is reduced in the presence of taxol-stabilized microtubules; our interpretation of these results, however, differs from theirs. We would like to point out that Sontag *et al.* (60) collected PKA-phosphorylated Tau, which was still bound to microtubules, by co-sedimentation with the microtubules, and dephosphorylated them after stabilization of microtubules with taxol. They argued that microtubules inhibit PP2A activity using myosin-light chain as a substrate that does not bind to microtubules. In our experiments, however, dephosphorylation of ΔMTB or NF-L, both of which do not bind microtubules, proceeded as fast as soluble Tau even in the presence of microtubules, suggesting that Tau becomes resistant to dephosphorylation by binding to microtubules. The difference may be derived from the protein phosphatase fraction used; we used rat brain extracts that contain various forms of PP2A, including ABαC complex, whereas Sontag *et al.* (60) used purified ABαC complex. In either case, both datasets suggest that dephosphorylation of Tau is suppressed in the presence of microtubules regardless of whether Tau is phosphorylated by PKA or Cdk5. We think that the suppression is caused by a conformational change in Tau upon microtubule binding, which evades PP2A recognition. Tau has been thought to lack a defined conformation, but some folding of Tau also has been reported (61, 62). It remains unknown, however, whether Tau changes conformation upon binding to microtubules. A recent NMR study revealed two tubulin binding motifs in the proline-rich region flanking the GSK3 phosphorylation site Ser-231 and Cdk5 phosphorylation site Ser-235 (63). As such, it is highly possible that accessibility of kinases or phosphatases to these phosphorylation sites is affected by microtubule binding. Notably, dephosphorylation of Tau bound to microtubules may reflect the situation of PHF Tau, which is resistant to dephosphorylation by protein phosphatases (27). If PHF Tau acquires a conformation similar to that of Tau on microtubules, then investigation of microtubule-dependent suppression of dephosphorylation may help to elucidate the mechanism by which PHF Tau remains hyperphosphorylated.

Taken together, our results suggest a model for how mutant Tau remains highly phosphorylated in the brains of FTDP-17 patients. The phosphorylation state of most FTDP-17 mutants is similar to P301L rather than R406W. Therefore, high phosphorylation state of most mutants may be maintained by a reduced level of dephosphorylation by PP2A. Mutant Tau has a tendency to aggregate irreversibly, resulting in greater resistance to dephosphorylation, leading to hyperphosphorylation. And what of R406W, which appears to bind microtubules with higher affinity than other mutants in cells (52). Therefore, the R406W mutant Tau may undergo a conformational change, similar to other mutants, upon which dephosphorylation becomes insensitive to Pin1. Phosphorylated R406W on microtubules may aggregate with itself or with phosphorylated WT Tau. Interaction between phosphorylated Tau molecules on microtubules may induce oligomerization or PHF-like aggregates that would be relatively resistant to dephosphorylation. In the case of WT Tau, association with microtubules also may